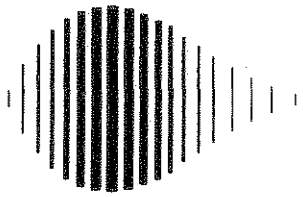

NATIONAL CENTER FOR EARTHQUAKE
ENGINEERING RESEARCH
State University of New York at Buffalo

OPTIMAL PLACEMENT OF ACTUATORS FOR STRUCTURAL CONTROL

by

F. Y. Cheng and C. P. Pantelides
Department of Civil Engineering
University of Missouri-Rolla
Rolla, Missouri 65401

Technical Report NCEER-88-0037

August 15, 1988

This research was conducted at the University of Missouri-Rolla and was partially supported by the National Science Foundation under Grant No. ECE 86-07591.

NOTICE

This report was prepared by the University of Missouri-Rolla as a result of research sponsored by the National Center for Earthquake Engineering Research (NCEER). Neither NCEER, associates of NCEER, its sponsors, the University of Missouri-Rolla, nor any person acting on their behalf:

a. makes any warranty, express or implied, with respect to the use of any information, apparatus, method, or process disclosed in this report or that such use may not infringe upon privately owned rights; or

b. assumes any liabilities of whatsoever kind with respect to the use of, or the damage resulting from the use of, any information, apparatus, method or process disclosed in this report.

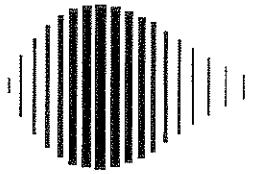

OPTIMAL PLACEMENT OF ACTUATORS FOR STRUCTURAL CONTROL

by

F.Y. Cheng[1] and C.P. Pantelides[2]

August 15, 1988

Technical Report NCEER-88-0037

NCEER Contract Number 87-2005

NSF Master Contract Number ECE 86-07591

1 Curators' Professor, Dept. of Civil Engineering, University of Missouri-Rolla
2 Assistant Professor, Dept. of Civil Engineering, University of Missouri-Rolla

NATIONAL CENTER FOR EARTHQUAKE ENGINEERING RESEARCH
State University of New York at Buffalo
Red Jacket Quadrangle, Buffalo, NY 14261

PREFACE

The National Center for Earthquake Engineering Research (NCEER) is devoted to the expansion and dissemination of knowledge about earthquakes, the improvement of earthquake-resistant design, and the implementation of seismic hazard mitigation procedures to minimize loss of lives and property. The emphasis is on structures and lifelines that are found in zones of moderate to high seismicity throughout the United States.

NCEER's research is being carried out in an integrated and coordinated manner following a structured program. The current research program comprises four main areas:

- Existing and New Structures
- Secondary and Protective Systems
- Lifeline Systems
- Disaster Research and Planning

This technical report pertains to Program 2, Secondary and Protective Systems, and more specifically, to protective systems. Protective Systems are devices or systems which, when incorporated into a structure, help to improve the structure's ability to withstand seismic or other environmental loads. These systems can be passive, such as base isolators or viscoelastic dampers; or active, such as active tendons or active mass dampers; or combined passive-active systems.

In the area of active systems, research has progressed from the conceptual phase to the implementation phase with emphasis on experimental verification. As the accompanying figure shows, the experimental verification process began with a small single-degree-of-freedom structure model, moving to larger and more complex models, and finally, to full-scale models.

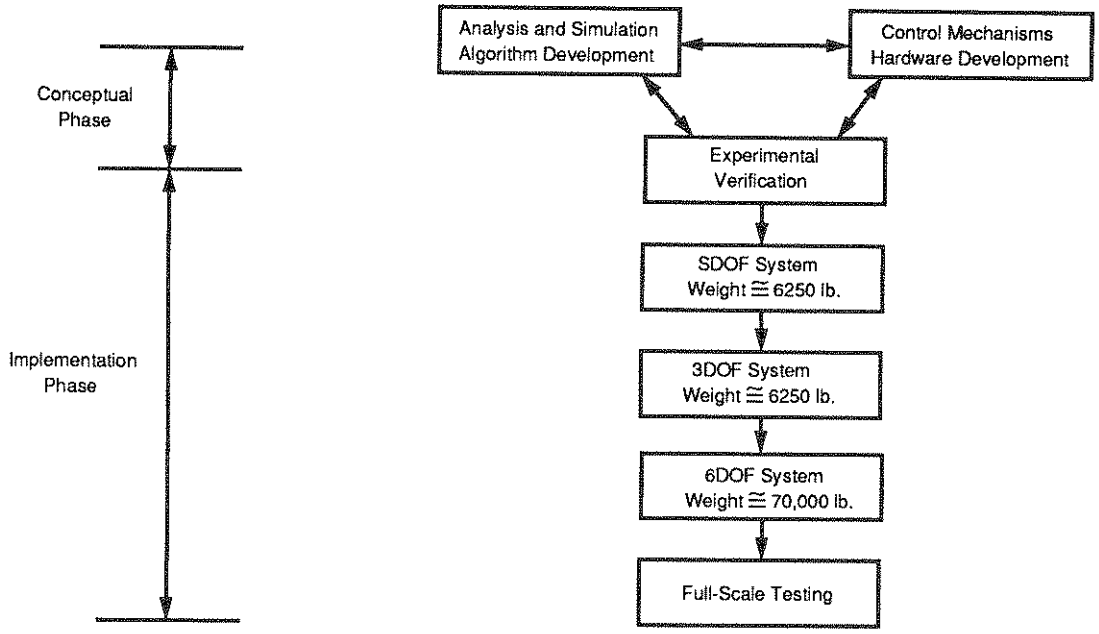

Active tendon systems have been studied extensively both analytically and experimentally. When they are applied to complex structures such as tall buildings, the problem of tendon placement becomes important from the point of view of maximum effectiveness and, at the same time, minimum power and system requirements. This report proposes a method of solution to this optimal placement problem. The method uses an empirical procedure to find the optimal actuator placement by maximizing a controllability performance index. It is shown that it is in agreement with the method of using control energy and response performance indices, but has significant computational advantages.

ABSTRACT

It is believed that in the application of structural control to seismic structures certain locations are advantageous for placement of the actuators. The term optimal actuators placement reflects upon the reduction of the structure's response while using the minimum control effort. By varying the location of the actuators and the amount of control force exerted by each controller, different dynamic responses are obtained in the simulation.

Two methods for selecting these optimal locations included in a previous report [ref. 9] are integrated. The first method utilizes the minimization of a control energy performance index. The second method uses a minimum response performance index as the criterion. A new method is proposed which uses an empirical procedure to find the optimal locations by maximizing a controllability performance index. Using modal responses and earthquake spectra, the optimal locations are determined by selecting the floors with maximum optimal locations index. The three methods are compared and simulation studies are carried out using various earthquake records.

TABLE OF CONTENTS

LIST OF ILLUSTRATIONS

LIST OF ILLUSTRATIONS (CON'T)

LIST OF TABLES

SECTION 1

INTRODUCTION

The application of structural control to civil engineering structures subjected to severe earthquakes implies that the performance and serviceability of the structure remain within prescribed limits. Thus the structure is protected and catastrophic results are prevented. Structural control can be achieved using passive control devices, active control devices, or a combination of passive and active devices.

Active control devices require external energy for their operation. The cost of the active control device and the power required to operate and maintain it become significant factors in the determination of an effective protection system. Thus the question of the number and optimal placement of the active control devices becomes important. The control devices under consideration are active tendons [refs. 1, 2] and jet thrusters [ref. 3]. Implementation of these devices can be accomplished using various active control algorithms.

The topic of optimal actuators placement or determination of optimal locations has been addressed by various researchers. The concept of obtaining the optimal locations by minimizing a performance index of control energy was studied by Martin and Soong [ref. 4]. Another method developed by Laskin [ref. 5] uses a scalar measure, the degree of controllability, whose primary importance obtains from its usefulness as a criterion for control actuator placement on large multi-dimensional systems. Lindberg and Longman [ref. 6] developed a method based on an independent modal space control algorithm for open-loop or closed-loop control by minimizing the

actual control effort. The optimal number and placement of actuators considering possible failures was studied by Vander Velde and Carignan [ref. 7]. A method based on the interpretation of the functional relationship between the actuators and the modes of the structural system was presented by Obe [ref. 8]. The method was applied to a prismatic beam and a square plate.

The methodology developed in this report is based on a scalar measure of controllability, the controllability index. The basic idea behind the method is that an actuator is optimally located where the displacement response of the uncontrolled structure is largest. Response spectra are used to predict the response of the structure utilizing the modal shapes of the structural system. The method is compared with the criteria of minimum control energy and minimum response indices presented by the authors in a previous report [ref. 9]. Also included in the present report are the issues of how many modes need to be considered in the determination of optimal locations, as well as the effect of different earthquake records on the optimal locations.

SECTION 2

OPTIMAL ACTUATORS PLACEMENT FOR SEISMIC STRUCTURES

The question of optimal location of actuators is linked with that of controllability. A system is controlled at time (t_o) if it is possible to find some control which can transfer the initial state $Z(t_o)$ to the origin at some finite time ($t_1 > t_o$). If this holds true for all initial times (t_o) and all initial states $Z(t_o)$, the system is completely controllable. However this definition is limited, i.e. a system is either controllable or it is uncontrollable. It is desirable to consider the question: How controllable is the system? That is, a degree of controllability is sought.

The degree of controllability is defined by Laskin [ref. 5] by a controllability index. The criteria used are either fuel-optimal systems for large space structures or time-optimal systems. However the derivations are for structures subjected to an initial disturbance and not to earthquake-excited structures. A new method is developed based on the notion of a scalar measure of degree of controllability for earthquake excited structures.

2.1 Actuator Placement for Initial Conditions Problem

The state equation of a second order system subjected to an initial disturbance $\{Z(t_o)\}$ can be written as, [ref. 9]

$$\{\dot{Z}(t)\} = [A]\{Z(t)\} + [B]\{u(t)\} \tag{1}$$

where:

$\{Z(t)\}$ = state-vector of displacements and velocities

$[A]$ = plant matrix

$[B]$ = location of controllers matrix

$\{u(t)\}$ = control forces

The control objective is to drive the initial disturbed state to the origin, i.e. the well-known regulator problem. Limitation of the control effort is accomplished by the constraint on the control forces

$$|u_i^*(t)| \leq u_{maxi}, \qquad i = 1, \ldots, m \tag{2}$$

where:

u_{maxi} = saturation limit of the ith control force

m = number of controllers

The control objective is to be achieved with the least control energy (fuel) E^*, and in the least possible time T^*. Laskin [ref. 5] defines a "recovery region" for the specified E^* and T^* within which the control force must remain during the effort. If the system is uncontrollable this region will collapse, since there will be at least one direction in the state-space along which no initial state can be driven to the origin regardless of the value of E^* and T^*. Mathematically the recovery region can be defined as the set R,

$$R = [\{Z(t_o)\} \equiv \{u(t)\},\ t\varepsilon[0,T^*],\ |u_i(t)| \leq 1,$$

$$\text{for } i = 1, \ldots, m,$$

$$\sum_{i=1}^{m} \int_0^{T^*} u_{maxi}|u_i(t)|dt \leq E^* \text{ such that } \{Z(T^*)\} = \{0\}] \tag{3}$$

Thus the recovery region is defined as the volume in which every initial condition $\{Z(t_o)\}$ can be brought to the origin at time T^*, with a set of control forces $|u_i(t)| \leq 1$, and for which the total energy required for all m controllers from time 0 to T^* is less than or equal to E^*.

The degree of controllability (DOC) is thus equal to the lower limit of the length of the recovery region. In other words the DOC is a scalar measure of the recovery region, that determines the region's smallest dimension. Using this definition of DOC, one can investigate the optimal location of actuators such that the DOC given above is to be maximized. Then the location of the actuators will be optimized in the sense that it maximizes the smallest dimension of the recovery region.

As an example of the use of the DOC, consider the optimal location of an actuator on a simply supported beam. The modal equations are

$$\ddot{V}_j + \omega_j^2 V_j = [\Delta_j]^T \{u\} \quad j = 1, \ldots, n \tag{4}$$

where:

$\{u\}^T = \{u_1, u_2, \ldots, u_m\}$

$[\Delta_j]^T = [u_{max_1} \varphi_j(X_1), u_{max_2} \varphi_j(X_2), \ldots, u_{max_m} \varphi_j(X_m)]$

$\varphi_j(X_i) = \sin j\pi X_i$

X_i = normalized distance of ith actuator from simple support

ω_j = jth natural frequency

Following Laskin's derivation [ref. 5] with the aid of the definition of DOC, the optimal location of the actuator ($X_1 \varepsilon [0,1]$) is found by maximizing ρ,

$$\rho = \max \left[\min_j \frac{|\sin j\pi X_1|}{\omega_j N_j} \right] \tag{5}$$

where:

j = jth mode

N_j = modal weighting factor

It is interesting to note that for a single actuator, at least, the optimal location is completely independent of the saturation limit of the control force (u_{max_1}), the minimum time T^*, and minimum control energy E^*. This independence however is lost for the multiple actuator case [ref. 5]. Also note that the optimal location does depend on the modal weighting factors (weight the analyst assigns according to which mode contribution is significant) and the number of modes (n), the analyst deems sufficient to describe the response. For this example if n = 1, the optimal location is at the center of the beam. For n = 2 and the two modes equally weighted, the optimal location is at either end of the third point of the beam.

2.2 Controllability Index for Seismic Structures

From the results of Section 2.1, based on the theoretical derivations, it is obvious that the optimal placement of actuators for seismic structures has a unique difference from the initial conditions problem; the structure is now continuously under a forced vibration state. The equations of motion for a controlled system become

$$[M]\{\ddot{Y}(t)\} + [C]\{\dot{Y}(t)\} + [K]\{Y(t)\} = \{P(t)\} + \{u(t)\} \tag{6}$$

The modal equations can be written as

$$\ddot{Y}_j + 2\zeta_j\omega_j\dot{Y}_j + \omega_j^2 Y_j = \frac{\{\varphi_j\}^T\{P(t)\} + \{\varphi_j\}^T\{u(t)\}}{\{\varphi_j\}^T[M]\{\varphi_j\}} \tag{7}$$

The presence of the first term on the RHS of Eq. (7) is the extra term that arises from the external excitation. However the mode-shapes are the same as before. Hence a combination of the effect of the mode shapes and the external excitation is needed to define the criterion of optimal locations for seismic structures. From Eq. (5) for the initial conditions problem, it is necessary to determine a good estimate of the influence of mode shapes on the response. In addition, the natural frequency is an important parameter. To establish the optimal locations index for earthquake excitation, one should use the seismic spectra as an implicit function of the individual modes.

The optimal locations criteria for seismic structures must take into consideration the following facts:

a) Lower modes are dominant in the response of earthquake excited structures
b) The control objective is to reduce the structural response and stabilize the seismic structure
c) The control effort in terms of control power available is limited
d) The structural response should not exceed certain thresholds for the safety and serviceability of the structure

Based on these premises the following assumptions are used in order to arrive at a meaningful optimal locations index for seismic structures:

a) Use the modal shapes of the uncontrolled structure to evaluate the influence of each mode
b) Use the response spectra of the actual earthquake when evaluating the response of the uncontrolled structure
c) Two different types of actuators can be used:

I) Jet thrusters (pulse control)

II) Active tendons

For each type of actuators a different form of optimal locations index OLI is defined for seismic structures.

From the theoretical derivation of Eq. (5) it is obvious that the modal shapes are an important parameter in the selection of the form of the OLI. Also it is obvious that the modes have to be weighted in a certain acceptable manner. As discussed previously, it is obvious that for seismic excited structures the earthquake spectra can be considered in the definition of the OLI. The question of minimum time T^*, is not as important for earthquake excited structures as for other applications. In particular in some aerospace applications time is extremely important. However seismic response is in effect governed by the duration of earthquake shocks. Minimum control energy, is handled in Section 3, independently of the definition of the OLI, as a check on the optimality of the solution.

Subject to the above facts and assumptions, the definition of the OLI for seismic structures must reflect the idea that an ideal location for a controller is where the displacement response of the uncontrolled structure is largest. For actuators that are jet thrusters (Type I) the OLI is defined as

$$\rho_a(X) = \max \sqrt{\sum_{j=1}^{n} [\varphi_j(X) Y_j(t)]^2} \qquad (8)$$

where:

$\rho_a(X)$ = OLI at location X (Type I)

X = percent of total height of building; $X \varepsilon [0,1]$

n = number of modes considered

$\varphi_j(X)$ = jth mode-shape

$Y_j(t)$ = jth mode, maximum response spectrum value

For actuators that are active tendons (Type II) the OLI is defined as

$$\rho_b(X) = \max \sqrt{\sum_{j=1}^{n} \left\{ \frac{\Delta[\varphi_j(X)]}{\Delta X} \; Y_j(t) \right\}^2} \qquad (9)$$

where:

$\rho_b(X)$ = OLI at location X (Type II)

$\Delta[\ ]$ = spatial difference of the quantity [ ], from position X_1 to position X_2

ΔX = difference in height $(X_2 - X_1)$

According to the stipulations outlined above, the best optimal location of controllers is thus defined to be the value of X, for which $\rho_a(X)$ or $\rho_b(X)$ are maximum. This definition is similar to that given by Eq. (5) in the sense that an index including the effect of modes, frequencies and earthquake spectra is maximized. The next best location is one for which $\rho_a(X)$ or $\rho_b(X)$ have the second maximum value, etc. Note that in Eq. (9) the algebraic difference of the mode-shapes is considered, since for active tendons the relative displacement between the floors is the critical parameter. The effect of the earthquake is taken care by the maximum spectrum value. The different modes are weighted in a root-mean-square fashion since the modal maxima do not occur at the same time.

Extensive discussion of the criteria developed in this section is given in the numerical examples following Section III.

2.3 Numerical Examples

2.3.1 Example 1: Type I Actuators--Cantilever Structure

The procedure outline in Eq. (5) is modified for this problem to handle the cantilever structure of Figure 2-1. According to Laskin's procedure, the optimal location for a single actuator is found by maximizing

$$\rho = \max \left[\min_j \frac{|\varphi_j(X_1)|}{\omega_j N_j} \right] \tag{10}$$

where:

$\varphi_j(X_1)$ = jth mode shape

Now the closed-form solution of the frequencies and mode-shapes of a cantilever is given by

$$1 + \cos aL \cosh aL = 0$$

$$a^4 = \frac{\omega^2 \bar{m}}{EI}$$

$$\varphi_j(X_1) = [\sin (aL)X_1 - \sinh (aL)X_1 + \frac{(\sin aL + \sinh aL)(\cosh (aL)X_1 - \cos (aL)X_1)}{(\cos aL + \cosh aL)}] \tag{11}$$

where

$\bar{m}$ = uniform mass

E = elastic modules

I = moment of inertia

L = height of structure

The first two natural frequencies are given by

$$\omega_1 = (1.8751)^2 \sqrt{EI/\bar{m}L^4} \qquad (12a)$$

$$\omega_2 = (4.6941)^2 \sqrt{EI/\bar{m}L^4} \qquad (12b)$$

The modal weighting factors can be defined in two ways:

(a) For energy equally distributed among the modes $N_j = 1/\omega_j$;

(b) If the lowest modes are the most susceptible to excitation then $N_j = 1/(\omega_j)^2$. Here for purposes of comparison with Laskin's results, set

$$N_j = \frac{1}{\omega_j} ; \qquad j = 1,2 \qquad (13)$$

and consider the first and second modes only. For a single actuator the results of using Eq. (10) are given in Table 2-I. A plot of ρ is given in Figure 2-2. The best location is at the top floor.

The proposed method of Eq. (8) is applied to the same structure for point actuators or jet thrusters. The following structural parameters are used: L = 96 ft, $\bar{m}$ = 0.08 kip-sec^2/ft^2, EI = 2.5x10^6 kip-ft^2. Using Eqs. (11) and (12) one can obtain ω_1 = 2.13 rad/sec, ω_2 = 13.37 rad/sec, and the corresponding first and second mode-shapes. The first and second-mode periods are 2.95 sec and 0.47 sec respectively. Using the N-S component of the 1940 El-Centro earthquake, the following maxima displacements were obtained from response spectra with 2% damping: Y_1 = 18.707 in., Y_2 = 2.926 in. The results for the controllability index of Eq. (8) are shown in Figure 2-3. The best location is at the top floor. The results of using Eq. (8) are given in Table 5-I in Appendix A. Again the best location is found to be the first floor. However there is a difference between the plots of Figures 2-2 and 2-3. The first mode dominates the response and

hence the overall shape of the optimal locations index of Figure 2-3 is heavily dependent on the first mode.

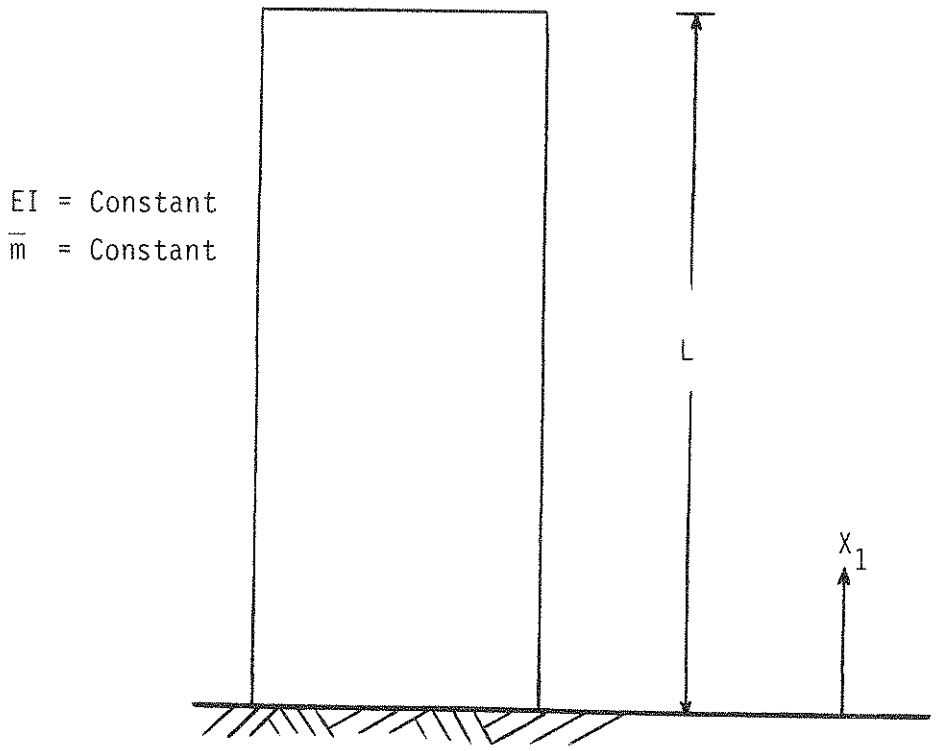

FIGURE 2-1 Cantilever Structure

TABLE 2-I CONTROLLABILITY USING LASKIN'S METHOD

X_1	$\|\varphi_1\|$*	$\|\varphi_2\|$	ρ = DOC
0.0	0.000	0.000	0.000
0.1	0.046	0.182	0.046
0.2	0.174	0.591	0.174
0.3	0.372	1.033	0.372
0.4	0.626	1.342	0.626
0.5	0.925	1.401	0.925
0.6	1.256	1.157	1.157
0.7	1.610	0.623	0.623
0.8	1.976	0.137	0.137
0.9	2.349	1.029	1.029
1.0	2.724	1.964	1.964

*|.| = absoultue value of quantity

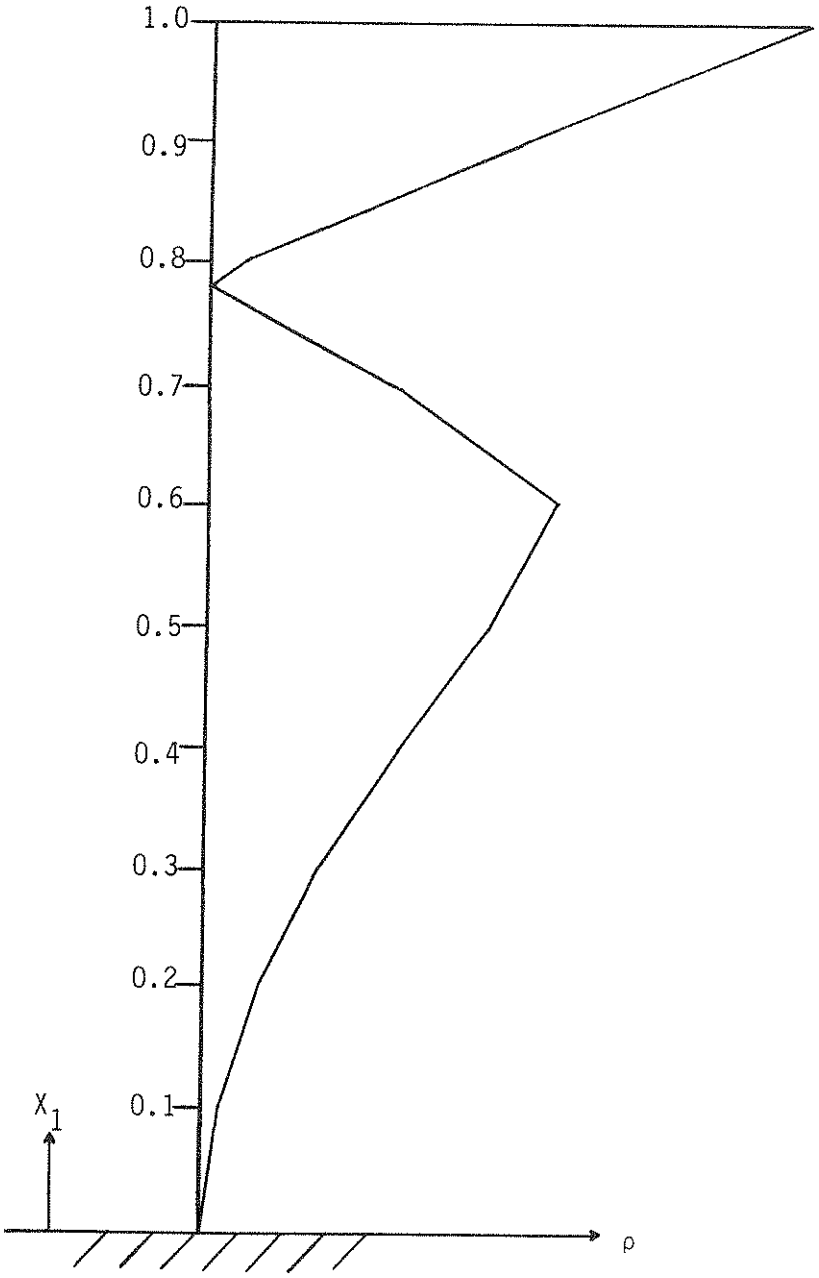

FIGURE 2-2 Laskin's Method For Optimal Locations for Cantilever Structure

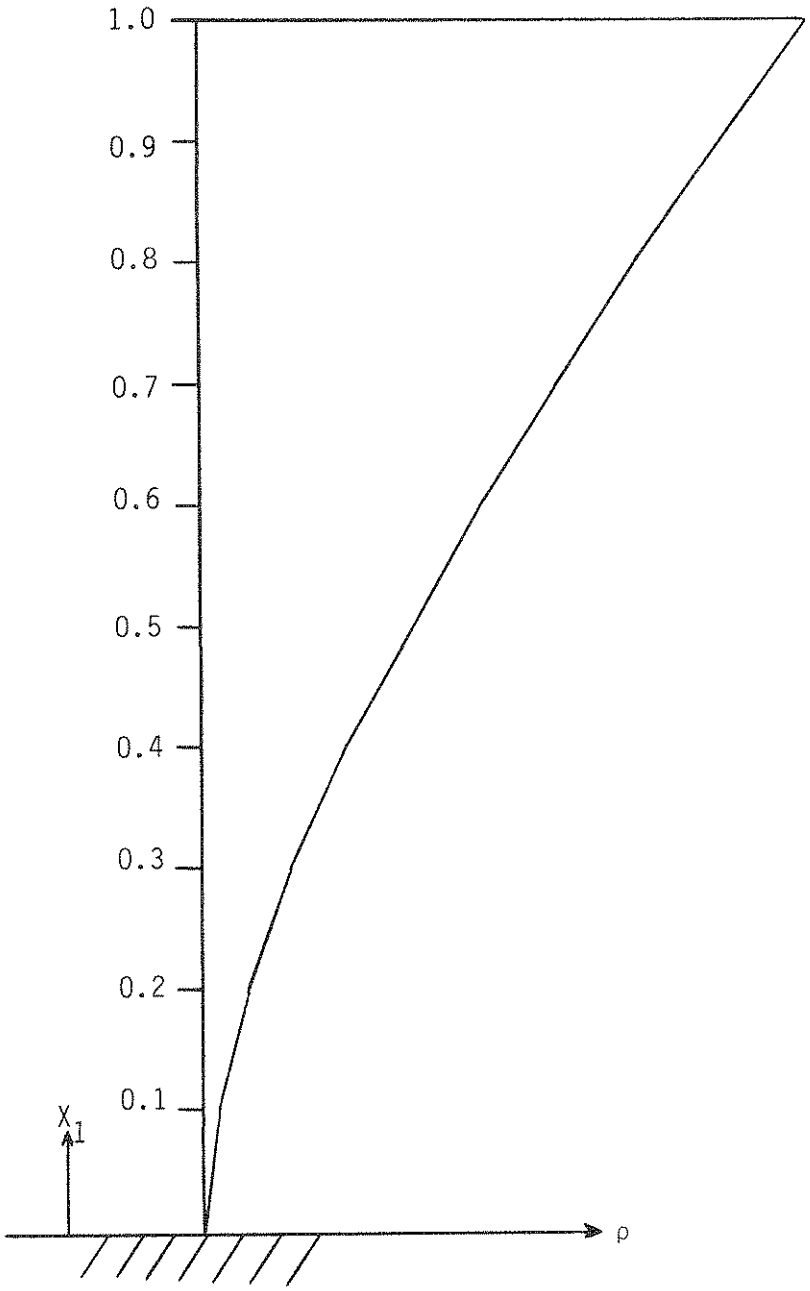

FIGURE 2-3 Proposed Method for Optimal Locations for Cantilever Structure Under Seismic Excitation

SECTION 3

OPTIMAL LOCATION OF ACTUATORS BASED ON PERFORMANCE CRITERIA

Any method attempting to determine the optimal locations of a limited number of actuators must answer the question: "How easy is it to control the system?" Thus we are seeking a quantitative measure of the notion of "ease." The performance criteria methods seek to define "ease" through a scalar measure of control energy and response performance. The methods consider an integral performance index for control energy and an integral performance index for displacement as well as velocity response. The disadvantage of the performance criteria methods is that their use is based on a trial and error procedure. The locations must be assumed and then the minimum performance criteria indices evaluated. The combinations of actuator locations that need to be checked become large for tall buildings. Nevertheless the performance criteria indices are useful when comparing the different optimal locations found by the method of Section 2. Thus a minimum energy E^* check can be carried out to see whether indeed the optimal locations obtained from Eq. (9) have minimum E^*.

3.1 Formulation Based on Performance Criteria Indices

The optimal location of a limited number of controllers can be established by considering the following criteria:

a) minimization of control energy index

b) minimization of response index

For a tall building equipped with active tendons (Figure 3-1), the equation of motion of the combined structure-control system is given as, [ref. 9]

$$\dot{\{Z(t)\}} = [A]\{Z(t)\} + [B]\{u(t)\} + \{C\}\ddot{X}_g(t) \tag{14}$$

where:

$\{Z(t)\}$ = state vector of displacements and velocities

$[A]$ = plant matrix involving the structure's mass, stiffness and damping

$[B]$ = location of controllers matrix

$\{u(t)\}$ = vector of control forces

$\{C\}$ = excitation influence vector

$\ddot{X}_g(t)$ = earthquake acceleration

The location of the controllers with respect to the structure configuration is reflected by the entries in matrix [B] of state-equation, Eq. (14). When a certain floor is equipped with a controller, the elements of matrix [B] are changed to reflect the influence of the controller on the floors above and below it. When the floor is not equipped with a controller the respective entries in the [B] matrix are set equal to zero.

The control energy index and response index are defined as follows:

$$J_E = \int_0^{t_f} \{u(t)\}^T \{u(t)\}\, dt \tag{15}$$

$$J_R = \int_0^{t_f} \{Z(t)\}^T \{Z(t)\}\, dt \tag{16}$$

where:

J_E = control energy index

J_R = response index

t_f = final time

The control energy index, J_E, reflects upon the desire to minimize the control work performed by the controllers in their operation from time t = 0 to t = t_f. The response index, J_R, on the other hand reflects upon the desire to minimize the structural response in the time from t = 0 to t = t_f. If the chosen locations are to be truly optimal they should minimize both of these indices.

3.2 Interpretation of Performance Criteria Indices

The use of the performance criteria indices J_E, and J_R is limited to one of a checking role. The reason is that the indices have to be evaluated after a possible optimal choice has been made. But even when they are calculated, it may be that a certain choice shows that the control energy index for this choice is higher than another choice, but the response index is less. So how is the judgement to be made? In order to answer this question and also to show the optimality of a choice over a broad range of control forces, a plot of the response index over the control energy index is suggested. This plot is obtained by varying the elements of the [Q] and [R] matrices in the optimal control performance index, $J_p(t)$, defined as, [ref. 9]

$$J_p(t) = \{Z(t)\}^T[Q]\{Z(t)\} + \{u(t)\}^T[R]\{u(t)\} \qquad (17)$$

where:

[Q] = positive semidefinite weighting matrix

[R] = positive definite weighting matrix

When the elements of [Q] and [R] are changed different levels of control forces {u(t)} are obtained which changes the control energy index J_E and

consequently different responses are produced which changes the response index, J_R.

The application of the response-index vs. control energy index plot is illustrated in the numerical examples and it is very useful when trying to compare various location choices. As the performance index of Eq. (17) implies, the algorithm used to calculate the time-histories of the control forces and the response simulations is the instantaneous closed-loop critical-mode control algorithm [ref. 9].

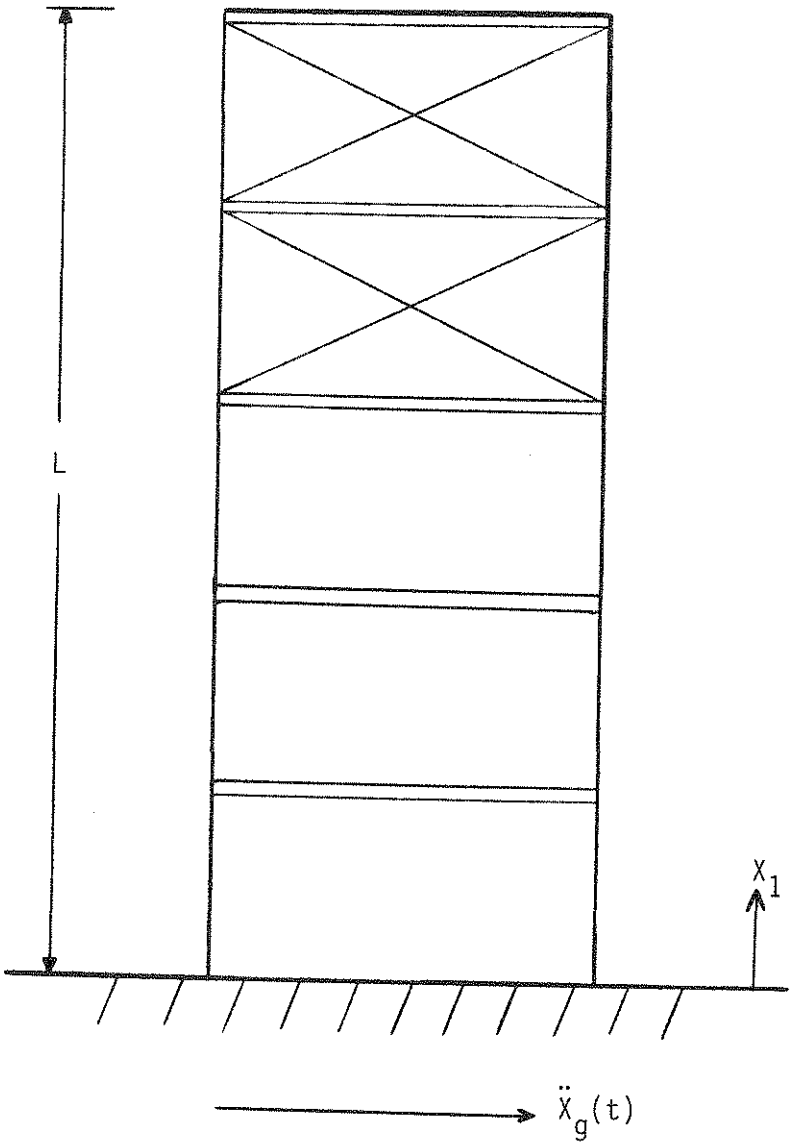

FIGURE 3-1 Building Equipped with Active Tendons

3.3 Numerical Examples

3.3.1 Example 2: Optimal Locations of Active Tendons

A fifteen-story shear building is studied for the optimal location of active tendon controllers on two of its floors. The structural properties of the building are as follows: floor stiffness k_i = 3000 k/in., m_i = 2 k-sec^2/in.: i = 1, ..., 15; damping = 3% critical. The weighting matrix [Q] is diagonal with $Q_{i,i}$ = 15000. The [R] matrix is varied in order to achieve different levels of control forces and hence different levels of control energy as described in Eq. (15). The controllability index of Eq. (9) is used to establish the optimal locations of the two active tendons. The first two natural frequencies of the structure without control are: ω_1 = 3.92 rad/sec, ω_2 = 11.73 rad/sec. These frequencies correspond to periods T_1 = 1.60 sec., and T_2 = 0.54 sec. Using the response spectra for the El-Centro 1940, N-S component, the following maximum response values are obtained: Y_1 = 0.439 ft, Y_2 = 0.265 ft. The first two modes are considered in evaluating Eq. (9) and the procedure is shown in Table 3-I. The mode shapes of the first two modes are given in Figure 5-1 in Appendix A. A plot of the controllability index $\rho_b(X)$ of Eq. (9) for the present example is shown on Figure 3-2. From Table 3-I and Figure 3-2 it can be seen that the first and second floor locations have maximum $\rho_b(X)$; hence they are chosen as the optimal locations. A comparison is made between two cases of locating the tendons. In case (A), floors one and two are equipped with active tendons, and in case (B) floors six and fifteen are equipped with active tendons. Figure 3-3 shows a plot of the two cases. The horizontal axis of the figure shows the control energy index of Eq. (15). The vertical

axis is the maximum displacement response of the fifteenth floor. As can be seen from Figure 3-3, case (A) is superior in reducing the maximum response for all control energy levels. Thus the minimum energy E^* criterion of controllability is automatically satisfied by Eq. (9).

Two comparisons are made for the two cases (A) and (B), as shown on Figure 3-3. In the first comparison (1), the two cases have the same control energy index fixed at a level of 1.1×10^6 as shown in Figure 3-3. Figures 3-4 and 3-5 show the displacement response of the first and fifteenth story respectively for the fixed control energy level. It is observed that for the same amount of control energy, case (α) produces less response. Similar results are true for all the other response quantities and the other floors.

In the second comparison (2), the fifteenth story maximum displacement was made equal for both cases (A) and (B) at 6.16 in. as shown in Figures 3-3, and 3-6. Then the two sets of the pairs of control forces required, were studied for cases (A) and (B). Figure 3-7 compares the first-story control force of case (A) and the sixth-story control force of case (B). It can be seen that case (A) requires less control force. Figure 3-8 compares the second-story control force of case (A) with the fifteenth-story control force of case (B). Again it can be seen that case (A) requires less control force. The control energy index for case (A) is 0.28×10^6, as compared to 1.1×10^6 for case (B). Hence case (A) is superior from both the response and control energy points of view. It is obvious that the minimum energy E^* criterion of controllability has been satisfied by Eq. (9) in this respect.

TABLE 3-I OPTIMAL CONTROLLER LOCATIONS

Floor	X	1st mode $\varphi_1(x)$	2nd mode $\varphi_2(x)$	$\Delta\varphi_1/\Delta x$	$\Delta\varphi_2/\Delta x$	$\rho_b(x)$
1	.067	.026	-.076	.390	1.140	10.60
2	.133	.051	-.145	.375	1.035	9.76
3	.200	.076	-.201	.375	.840	8.45
4	.267	.100	-.238	.360	.555	6.59
5	.333	.123	-.254	.345	.240	5.01
6	.400	.145	-.246	.330	.120	4.52
7	.467	.165	-.216	.300	.450	5.42
8	.533	.184	-.165	.285	.765	7.27
9	.600	.201	-.100	.255	.975	8.60
10	.667	.216	-.026	.225	1.110	9.47
11	.733	.228	.051	.180	1.155	9.65
12	.800	.238	.123	.150	1.080	8.97
13	.867	.246	.184	.120	.915	7.57
14	.933	.251	.228	.075	.660	5.43
15	1.000	.254	.251	.045	.345	2.86

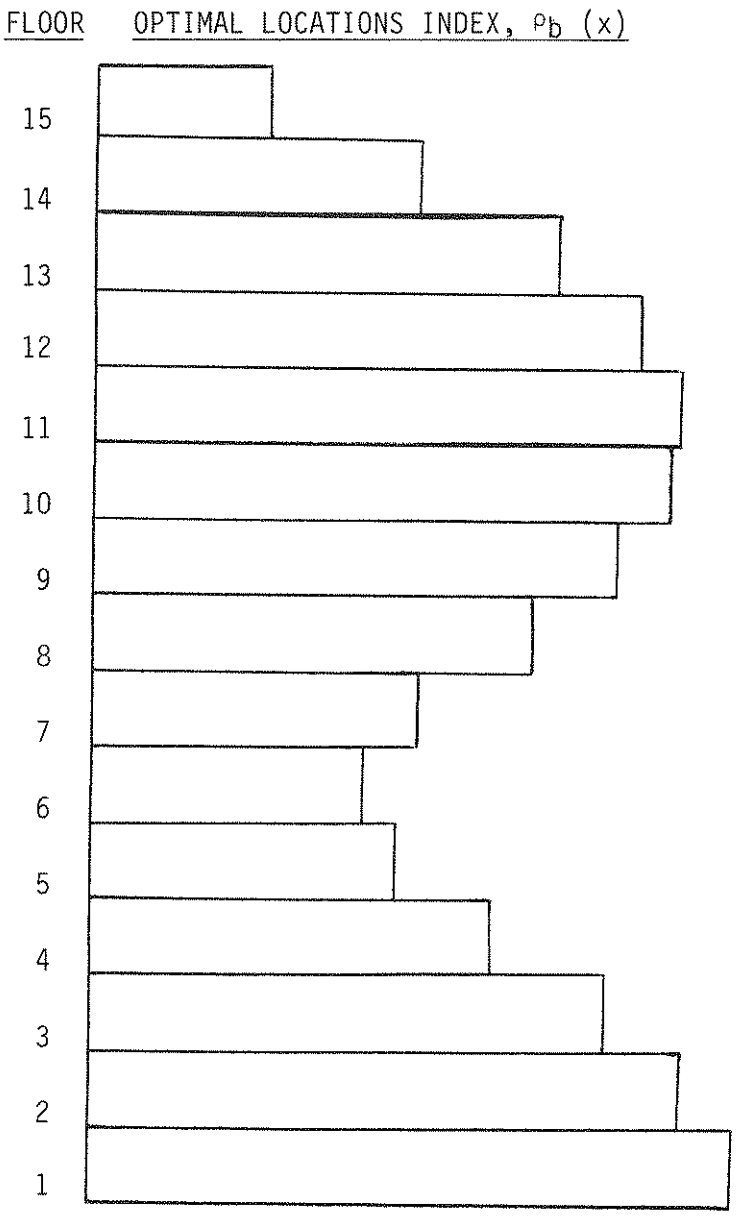

FIGURE 3-2 Optimal Locations of Active Tendons for Fifteen-Story Seismic Structure

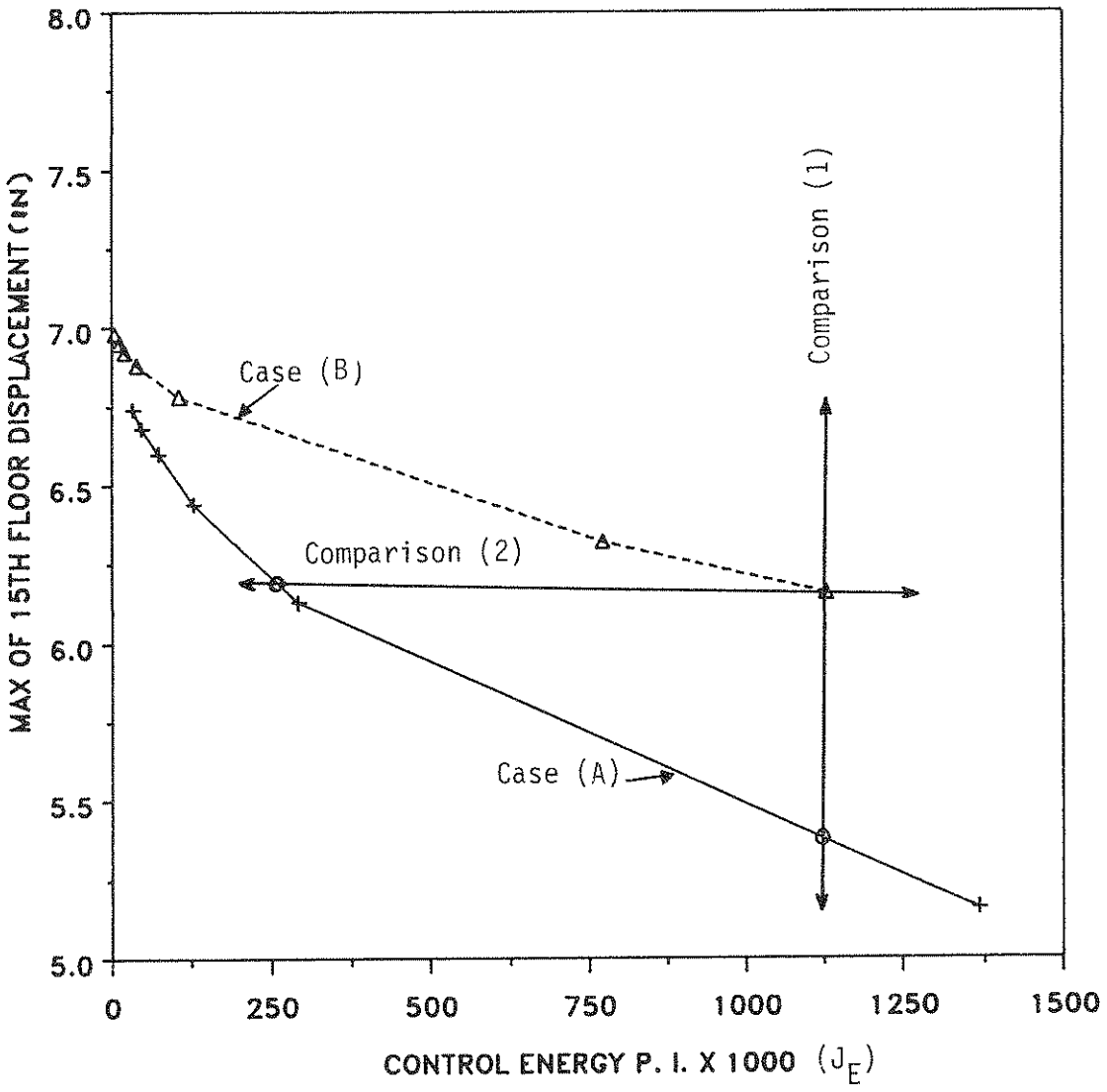

FIGURE 3-3 Comparison of Cases (A) and (B)

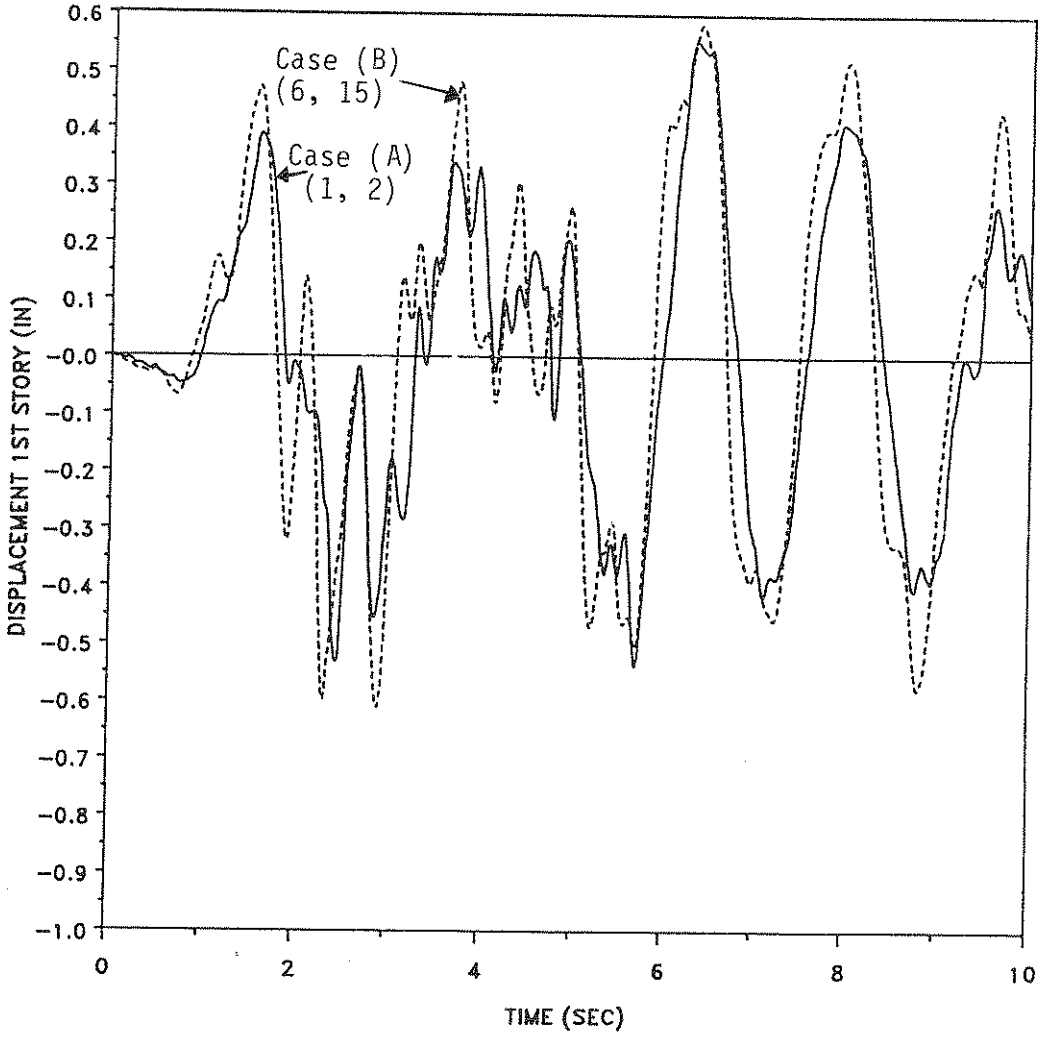

FIGURE 3-4 Displacement of 1st Story for Fixed Control Energy: Cases (A) and (B) of Comparison (1)

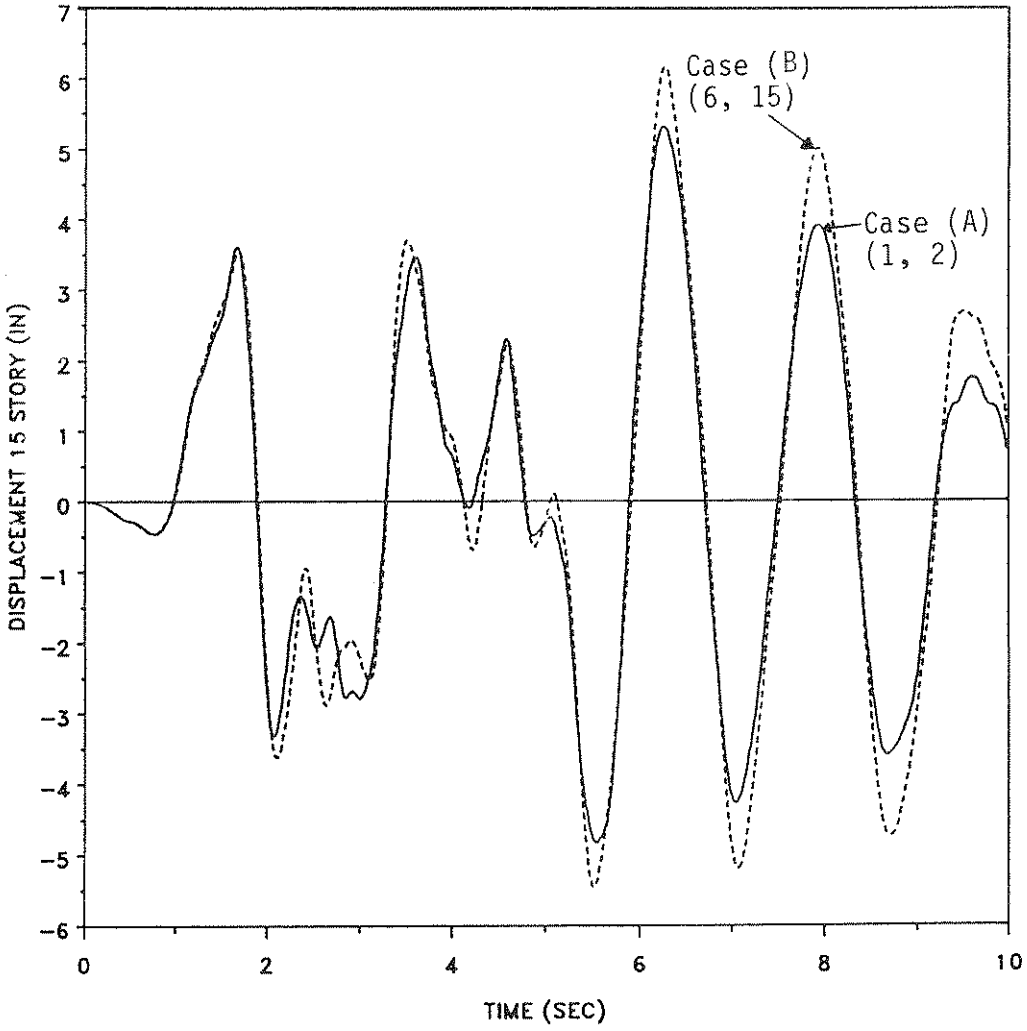

FIGURE 3-5 Displacement of 15th Story for Fixed Control Energy: Cases (A) and (B) of Comparison (1)

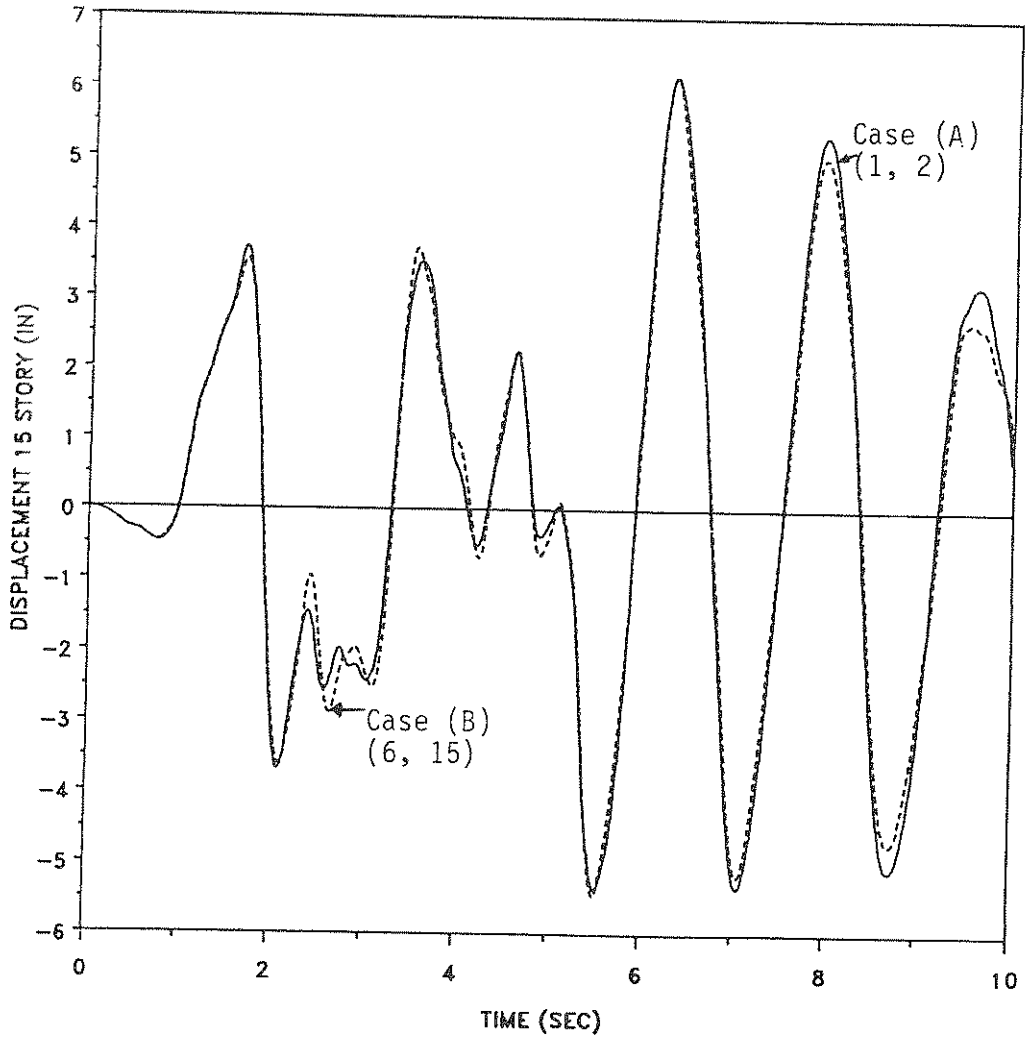

FIGURE 3-6 Equal Response of Fifteenth Story Displacement for Comparison (2)

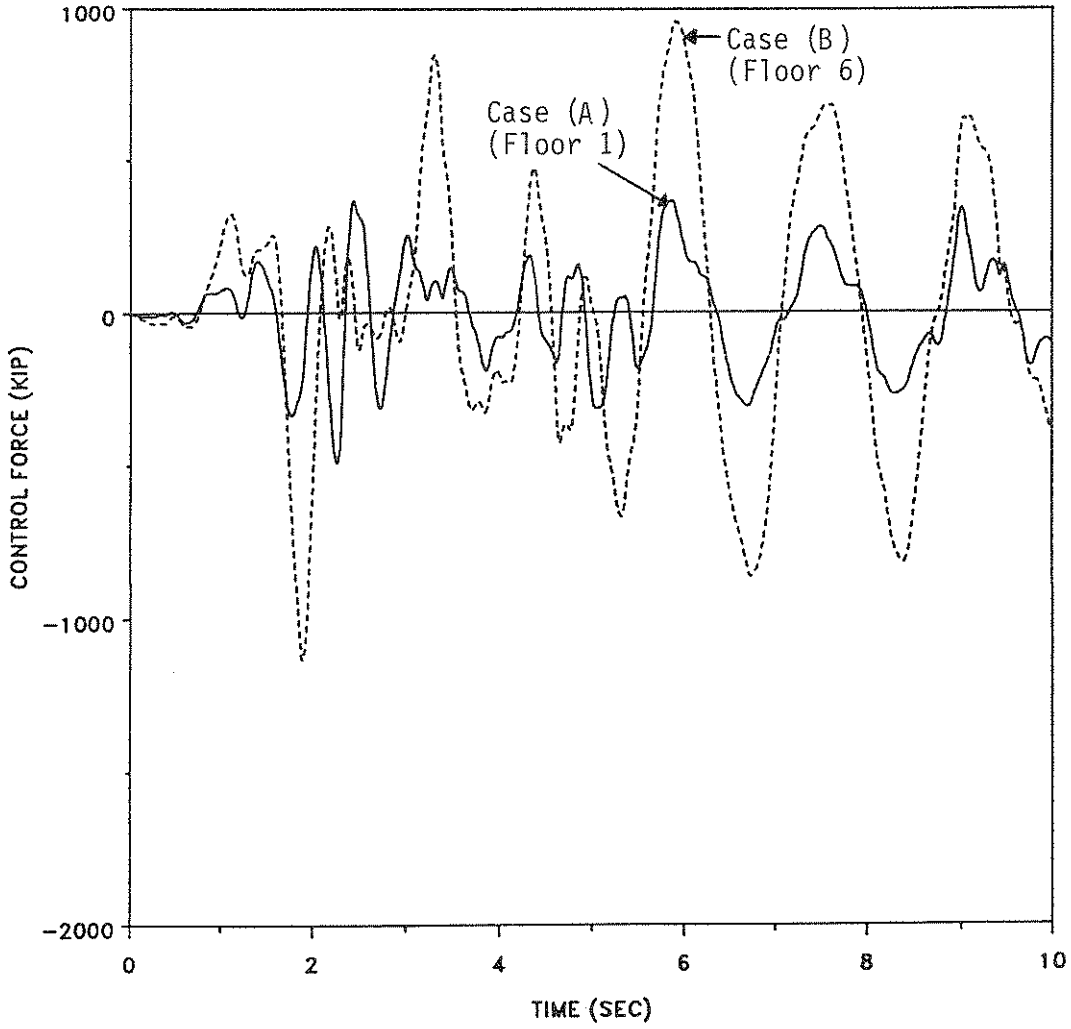

FIGURE 3-7 Control Forces for Comparison (2):
Case (A) 1st Story and Case (B) 6th Story

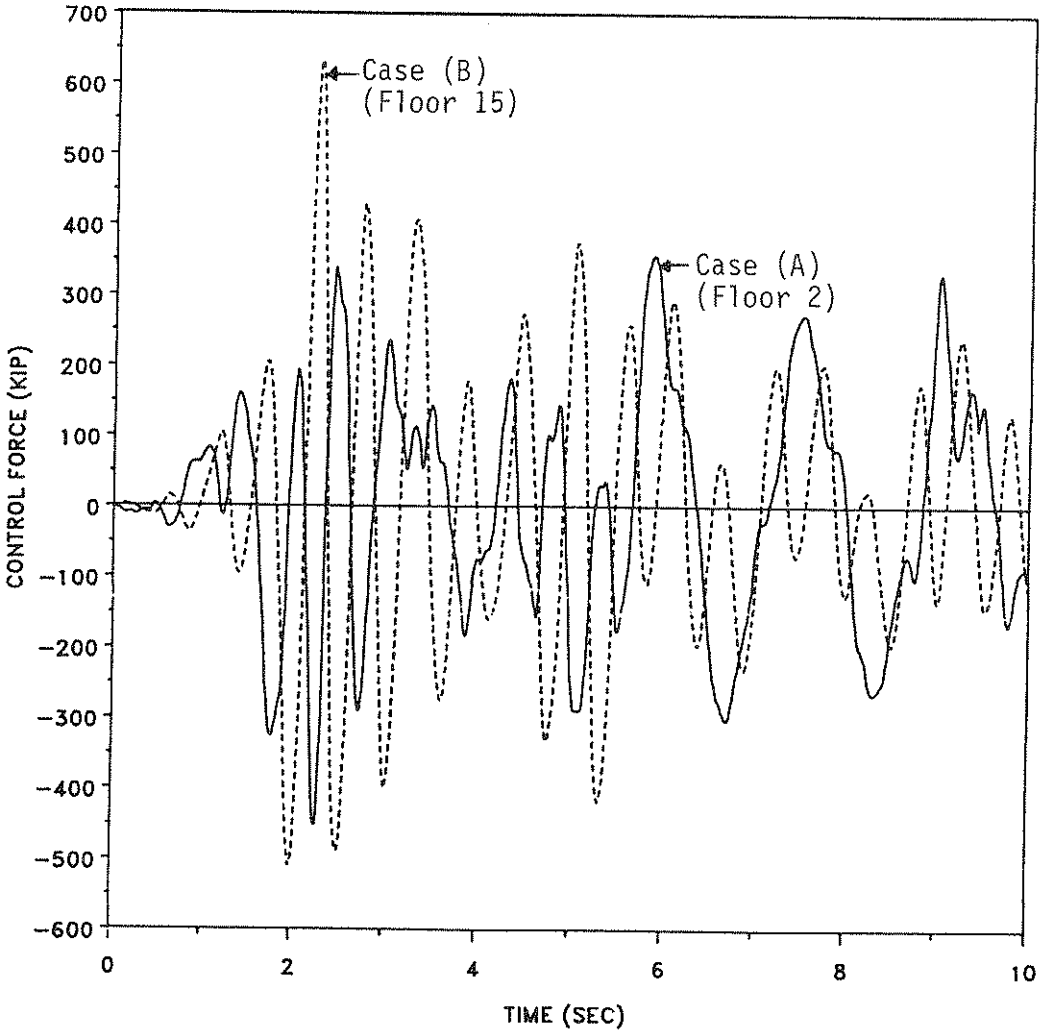

FIGURE 3-8 Control Forces for Comparison (2):
Case (A) 2nd Story and Case (B) 15th Story

3.3.2 Example 3: Effect of Controlled Mode-Shapes on Optimal Locations

It was noted in [ref. 9] that after a choice of optimal locations has been made, the modal shapes of the controlled structure are no longer the same as those of the uncontrolled structure. This can be observed from Eq. (14). When $\{u(t)\}$ is substituted in Eq. (14),

$$\{u(t)\} = -[k]\{Z(t)\} \tag{18}$$

where:

$[k]$ = constant gain

then the eigenvalues and eigenvectors of the closed-loop system are given by

$$[\bar{A}] = [A] - [k] \tag{19}$$

Hence the modal shapes of the controlled structure will be different. However we want to investigate whether this difference is significant enough to alter the optimal locations found using the method outlined in Section 2.

The closed-loop mode shapes of case (A) based on Eq. (19), were used to recalculate the controllability index $\rho_b(X)$, for the fifteen-story building of Example 2, and are given in Table 5-II of Appendix A. The results are shown in Figure 3-9. It can be observed that the first and second-story are still the optimal locations. The same conclusion was reached by using the mode-shapes of case (B).

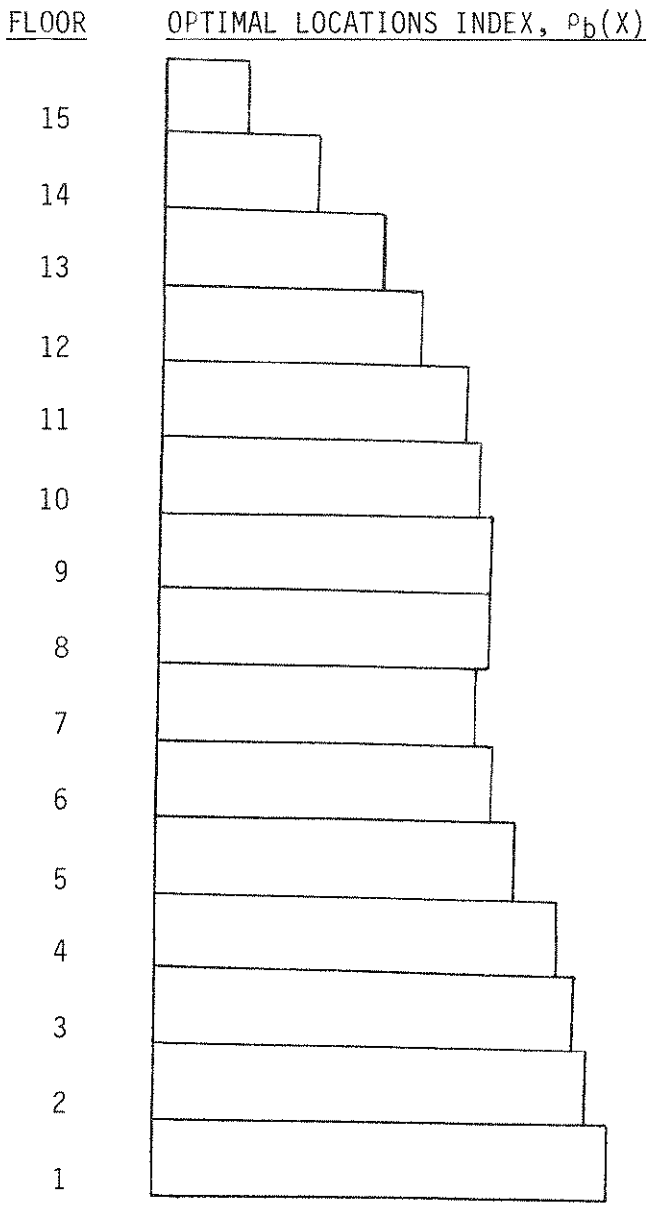

FIGURE 3-9 Controlliability Index for Fifteen-Story Seismic Structure using Mode-Shapes of Case (A)

3.3.3 Example 4: Effect of Different Earthquakes on Optimal Locations

The optimal locations determined for the fifteen-story building of Example 2, were found for the horizontal component, N-S direction, of the El-Centro 1940 earthquake. This example is to determine whether the locations found in Example 2 would still be optimal in the case of another earthquake. For the purpose of this study, the 1985 Mexico City earthquake shown in Figure 3-10 was used.

Judgement of whether the optimal locations will remain the same is made by observing the response spectra for the displacement of the two records, since this will be the only parameter that will change in Eq. (9). Figure 3-11 shows the two curves for 3% damping. It can be seen that the two curves though not identical are parallel for the range of periods of interest. Note that in calculating the optimal locations the relative and not the absolute magnitude of displacement response spectra is of importance. The fact that the response spectra are parallel will produce the same optimal locations. Thus it can be predicted that the locations found for El-Centro will still be optimal for the Mexico earthquake.

Calculation of the controllability index $\rho_b(X)$ for the Mexico earthquake, using the structure of Example 2 shows that case (A) is still optimal. In Figure 3-12 the indices of Eqs. (15) and (16) are shown for the Mexico earthquake for cases (A) and (B) of Example 2. It can be observed that for all levels of control energy index the response index for case (A) is less than that for case (B).

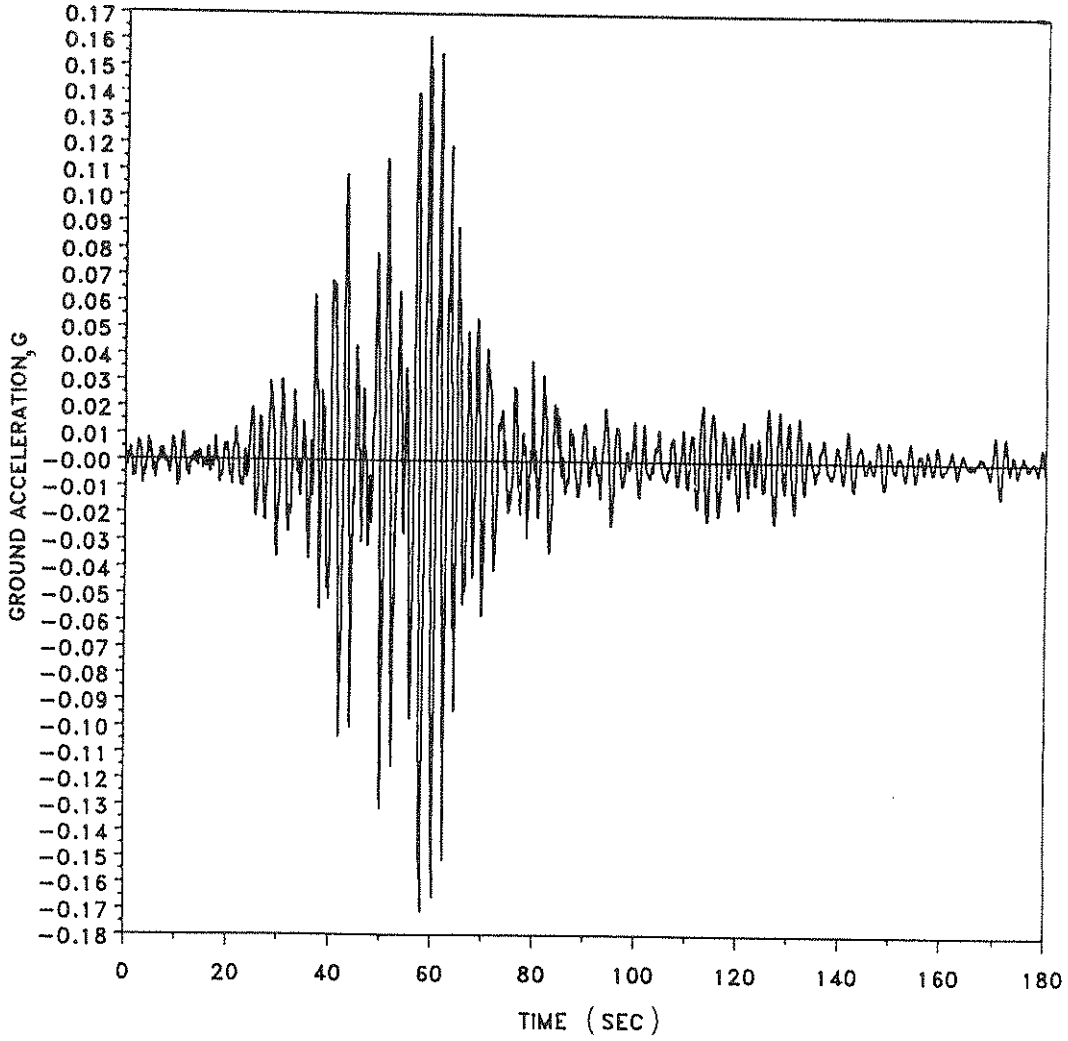

FIGURE 3-10 Acceleration Record of 1985 Mexico City Earthquake

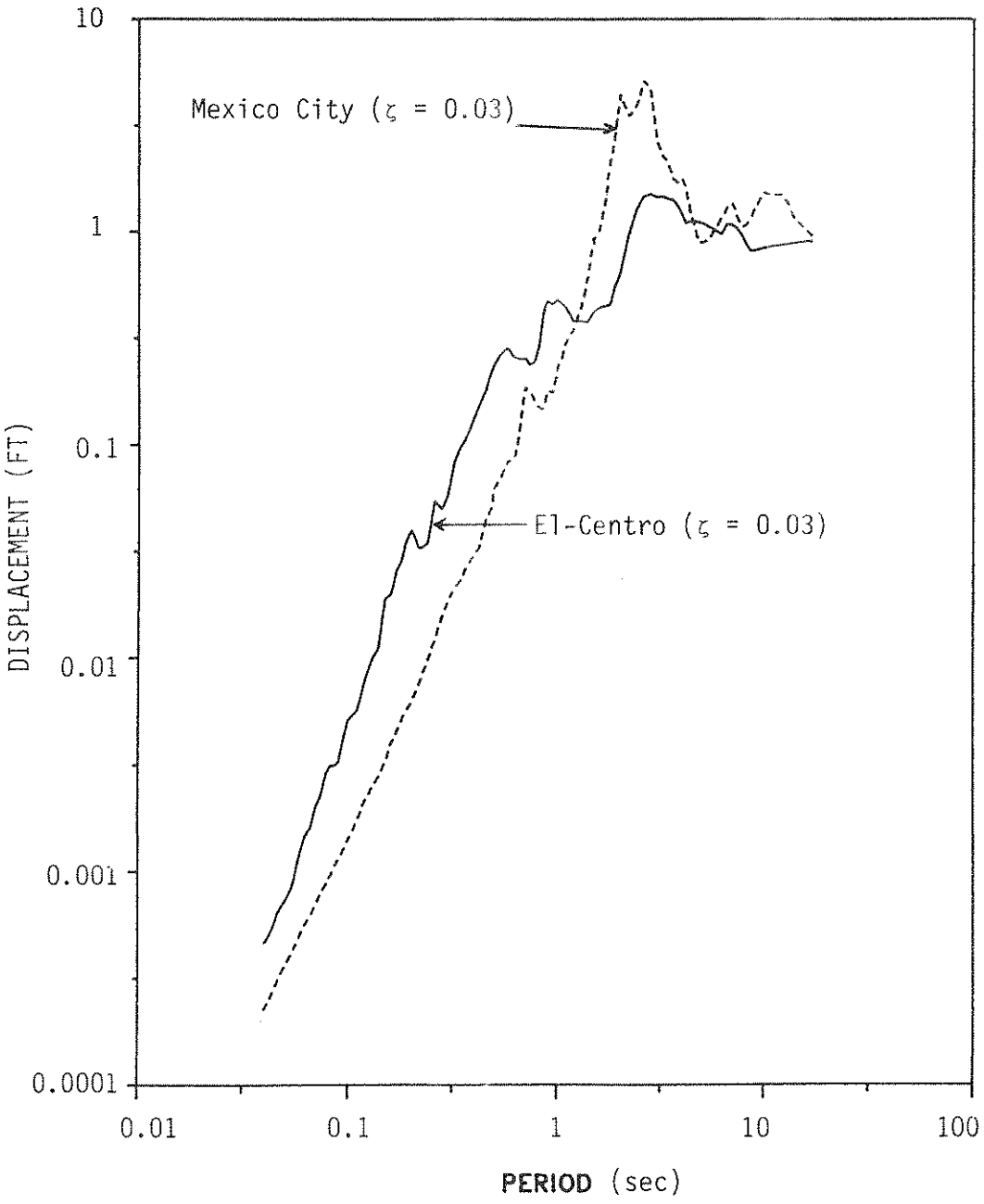

FIGURE 3-11 Comparison of Displacement Response Spectra for El-Centro 1940 and 1985 Mexico City Earthquakes

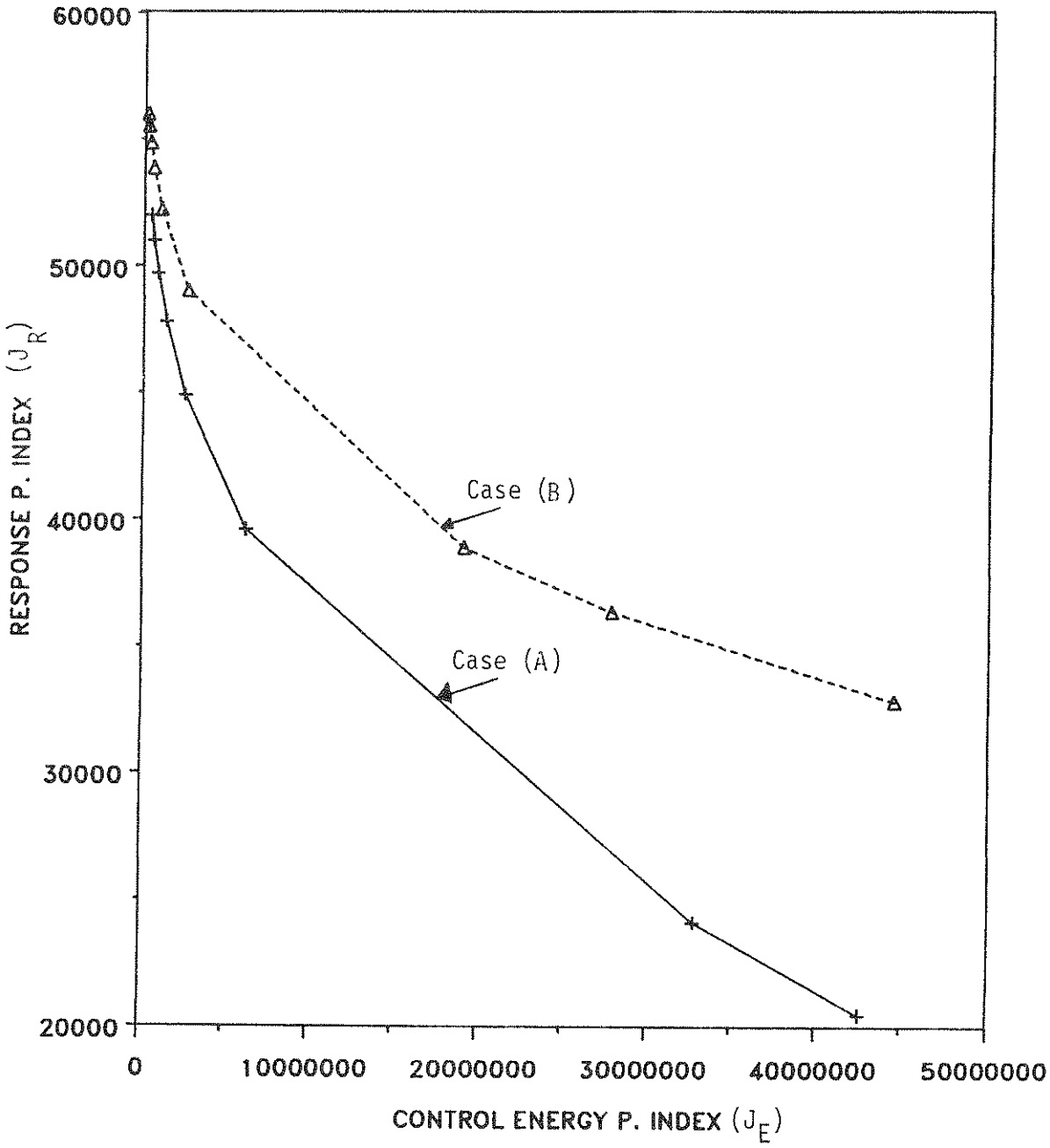

FIGURE 3-12 Control Energy and Response Performance Indices for the 1985 Mexico City Earthquake

3.3.4 Example 5: Variability of Optimal Locations with Structural Parameters

The structural parameters of the fifteen-story building of Example 2, are modified in this example, in order to observe whether or not the optimal locations found will be different from those found previously. Recall that in Example 2 the optimal locations were the first and second floor for the choice of two controllers. The structural parameters used in the present example are: k_1 = 3000 k/in., k_2 = 2750 k/in., k_3 = 2500 k/in., k_4 = 2250 k/in., k_5 = 2000 k/in., k_6 = 1750 k/in., k_7 = 1500 k/in., k_8 = 1250 k/in., k_9 = 1000 k/in., $k_{10} = k_{11} = k_{12} = k_{13} = k_{14} = k_{15}$ = 800 k/in.; m_i = 2 k-sec^2/in.; i = 1, ..., 15; damping = 3% critical. The weighting matrix is diagonal with $Q_{i,i}$ = 15000 as before. The first two natural frequencies of the structure without control are: ω_1 = 2.896 rad/sec., ω_2 = 7.635 rad/sec. which correspond to periods of T_1 = 2.17 sec. and T_2 = 0.82 sec. respectively. Using the response spectra for the El-Centro 1940, N-S component, the following maximum response values are obtained: Y_1 = 0.894 ft., Y_2 = 0.294 ft. The first two modes are considered in evaluating Eq. (9) and the procedure is shown in Table 3-II. The mode shapes of the first and second mode are given in Figure 5-2 of Appendix A. A plot of the controllability index of Table 3-II is shown on Figure 3-13. It can be seen that the first and second floor locations are no longer optimal; instead the optimal locations are the tenth and eleventh floor. A comparison of the first and second floor locations with the tenth and eleventh floor locations is carried out for the data of the present example. Figure 3-14 shows a comparison of the two cases in terms of the control energy and response performance indices. Clearly the tenth and eleventh floor choice is

superior at all energy levels. The 15th floor displacement response for the two cases is compared in Figure 3-15. The comparison is for equal control energy for both cases at the level of 2,475,000. This example demonstrates the fact that Eq. (9) will predict optimal locations correctly for a structure with different structural parameters. As is observed the optimal locations change because of the new periods, maximum spectral responses and mode-shapes of the new structure. However Eq. (9) is still valid.

TABLE 3-II OPTIMAL LOCATIONS FOR EXAMPLE 5

Floor	1st mode (φ_1)	2nd mode (φ_2)	$\Delta\varphi_1/\Delta x$	$\Delta\varphi_2/\Delta x$	$\rho_b(x)$
1	.013	-.042	.195	.630	.647
2	.027	-.086	.210	.660	.687
3	.042	-.130	.225	.660	.711
4	.059	-.173	.255	.645	.754
5	.077	-.211	.270	.570	.747
6	.097	-.240	.300	.435	.755
7	.120	-.255	.345	.225	.801
8	.145	-.250	.375	.075	.853
9	.174	-.214	.435	.540	1.067
10	.207	-.138	.495	1.140	1.412
11	.235	-.042	.420	1.440	1.441
12	.259	.060	.360	1.530	1.409
13	.277	.154	.270	1.410	1.222
14	.289	.225	.180	1.065	.897
15	.295	.263	.090	.570	.474

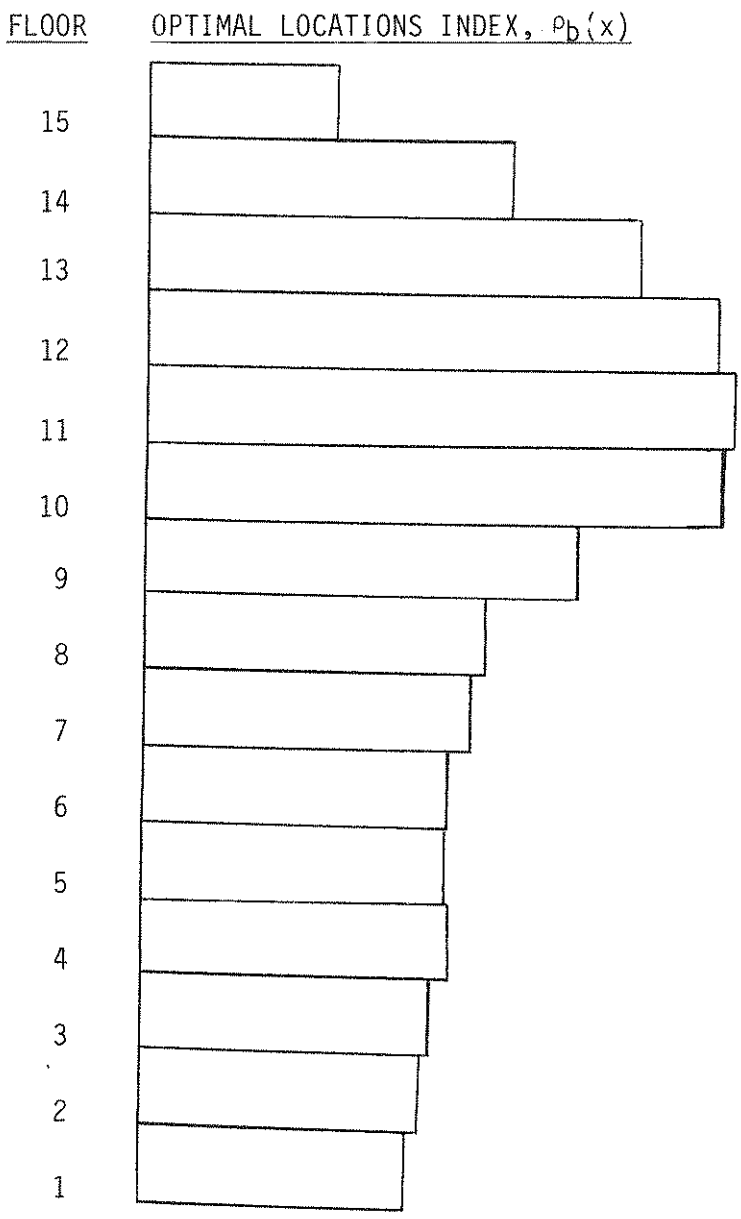

FIGURE 3-13 Optimal Locations Index for Example 5

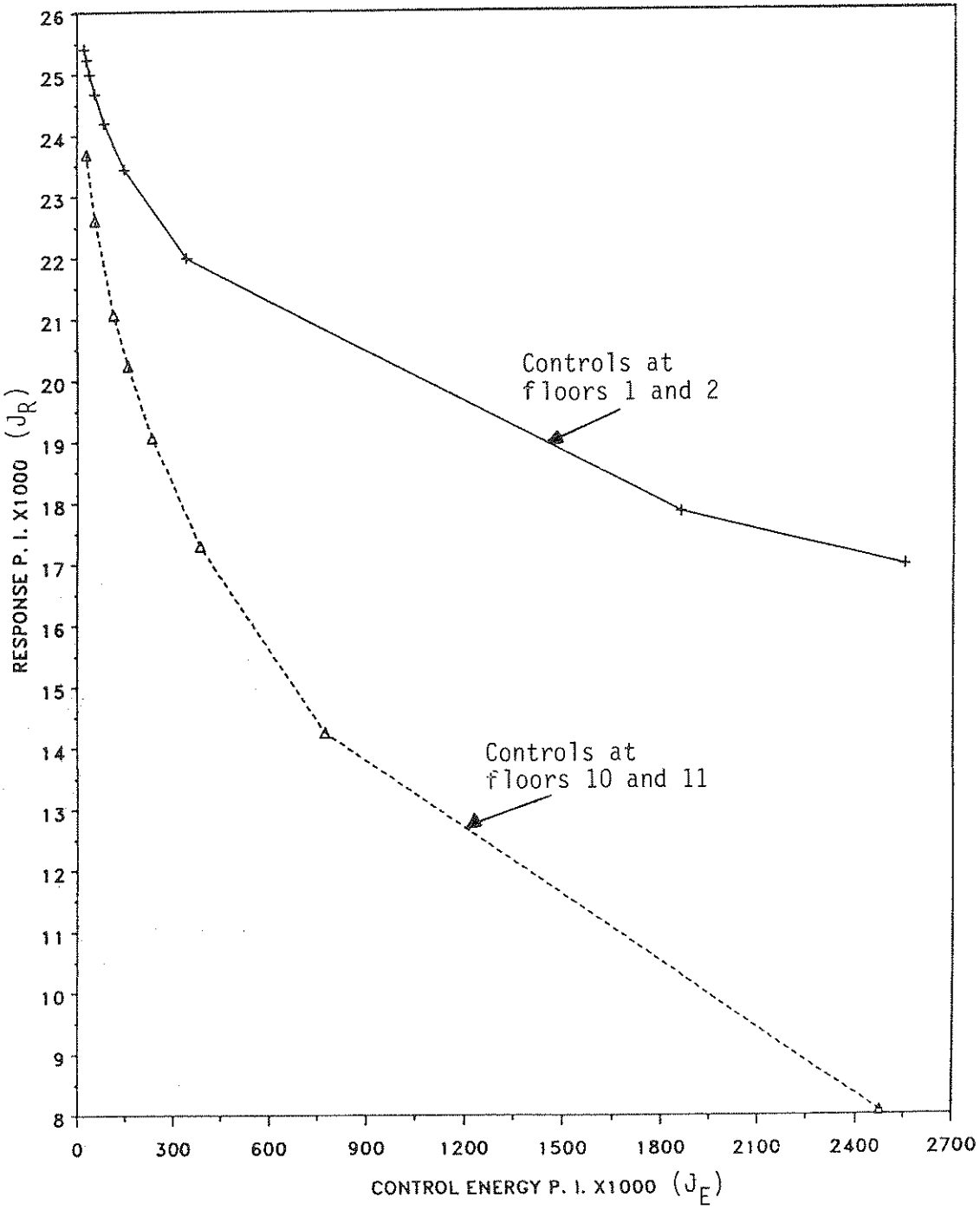

FIGURE 3-14 Control Energy and Response Performance Indices for First and Second Floor versus Tenth and Eleventh Floor Locations

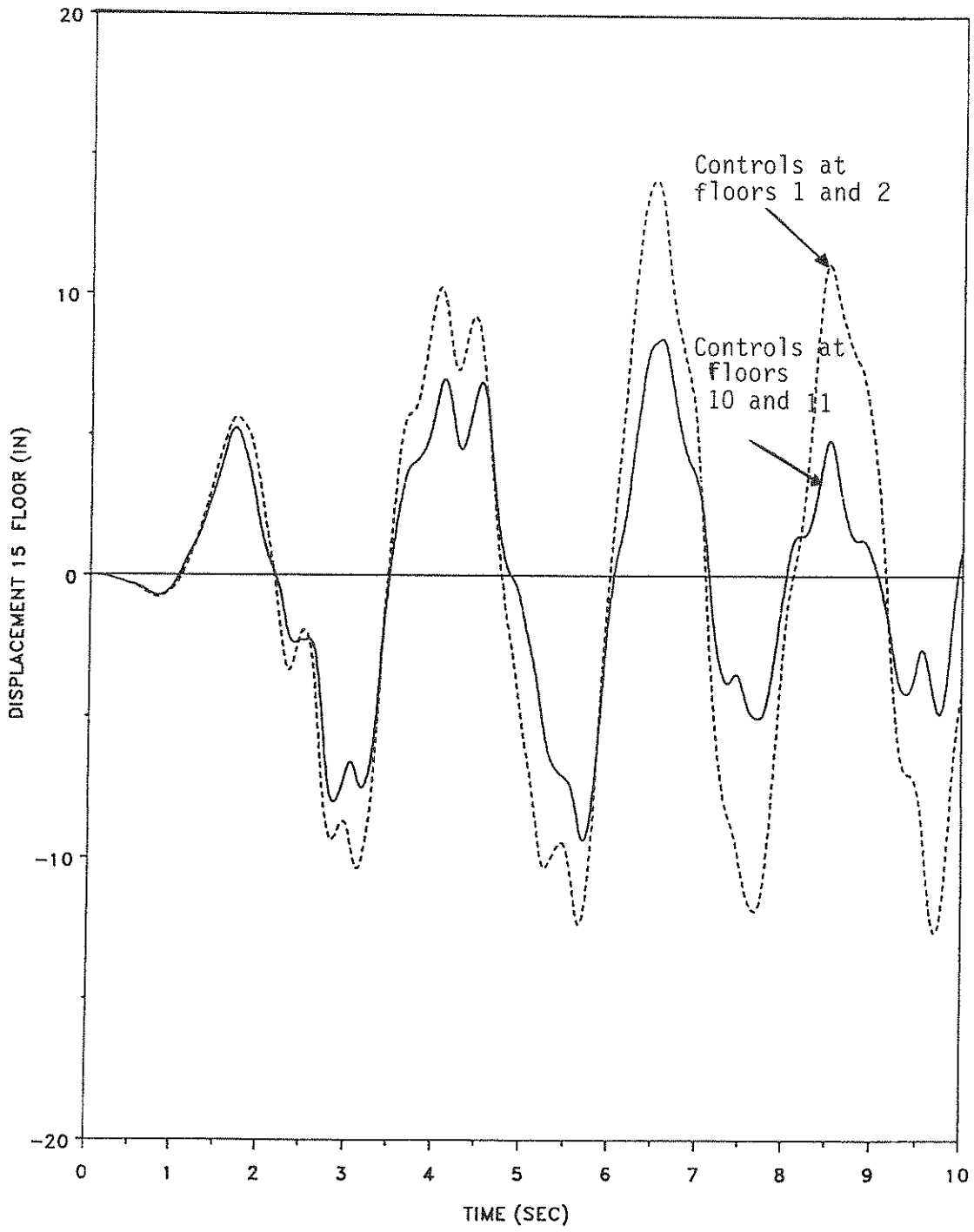

FIGURE 3-15 Comparison of Fifteenth Floor Displacement for First and Second versus Tenth and Eleventh Floor Locations

3.3.5 Example 6: Effect of Number of Modes Considered in Optimal Locations Selection

This example addresses the issue of the number of modes that are required in order for the method of Eq. (9) to yield the truly optimal locations of active controllers. The structural properties for the fifteen story building in this example are as follows: k_i = 300 k/in., m_i = 6 k-sec^2/in. for i = 1,..., 7; k_j = 200 k/in., m_j = 5 k-sec^2/in. for 8, ..., 15; damping = 3% critical. Two controllers are to be located optimally and starting out we consider only two modes. The first mode natural frequency is ω_1 = 0.732 rad/sec and the second frequency ω_2 = 1.954 rad/sec., with corresponding periods of T_1 = 8.58 sec. and T_2 = 3.22 sec. respectively. Using response spectra of the 1985 Mexico City earthquake (shown in Figures 3-10 and 3-11), the following maximum response values are obtained: Y_1 = 1.143 ft., Y_2 = 2.238 ft. The first two modes are then used to calculate the optimal locations index of Eq. (9) and the results are shown in Table 3-III. The mode-shapes of the first two modes are given in Figure 5-3 of Appendix A. A plot of the optimal locations index is given in Figure 3-16. It is seen that the tenth and eleventh floors are the optimal locations. Next three modes are considered in calculating the optimal locations index of Eq. (9), the first, second and third. The third mode natural frequency is ω_3 = 3.350 rad/sec. with corresponding period T_3 = 1.88 sec. The maximum response value is Y_3 = 2.684 ft. The optimal locations index is calculated using Eq. (9) and the results are shown on Table 3-IV. A plot of $\rho_b(X)$ for three modes is given in Figure 3-17. It can be seen that the optimal locations are no longer at the tenth and eleventh floors but are at the eighth and twelfth floors. The same result is obtained if one considers four modes, or

five modes, as shown on Table 3-IV, and Figure 3-17. Hence the eighth and twelfth floor locations are optimal. Figure 3-18 shows a comparison of two cases in terms of the control energy and response performance indices when only two modes are used. It can be seen that as predicted by $\rho_b(X)$ on Table 3-III and Figure 3-16, the optimal locations for two modes are floors ten and eleven. However a similar calculation considering five modes shown in Figure 3-19 shows that the optimal locations are really floors eight and twelve, as predicted by $\rho_b(X)$ on Table 3-IV and Figure 3-17. This example demonstrates the procedure for consideration of how many modes are required in using Eq. (9). In this case three modes are sufficient. In other situations more modes may need to be considered. The procedure can be terminated when an increase in the number of modes considered does not change the optimal locations.

TABLE 3-III OPTIMAL LOCATIONS FOR EXAMPLE 6 -- TWO MODES

Floor	1st mode (φ_1)	2nd mode (φ_2)	$\Delta\varphi_1/\Delta x$	$\Delta\varphi_2/\Delta x$	$\rho_b(x)$
1	.014	-.041	.21(.88)*	.62(.84)*	5.42
2	.024	-.078	.23(.96)	.56(.76)	5.14
3	.043	-.110	.21(.88)	.48(.65)	4.49
4	.056	-.133	.20(.83)	.35(.47)	3.60
5	.069	-.146	.20(.83)	.20(.27)	2.86
6	.081	-.148	.18(.75)	.03(.04)	2.19
7	.092	-.138	.17(.71)	.15(.20)	2.35
8	.108	-.108	.24(1.0)	.45(.61)	4.52
9	.122	-.068	.21(.88)	.60(.81)	5.27
10	.134	-.021	.18(.75)	.71(.96)	5.88
11	.145	.028	.17(.71)	.74(1.0)	6.05
12	.153	.074	.12(.50)	.69(.93)	5.49
13	.160	.113	.11(.46)	.59(.80)	4.74
14	.164	.141	.06(.25)	.42(.57)	3.23
15	.166	.156	.03(.13)	.23(.31)	1.80

* = Normalized

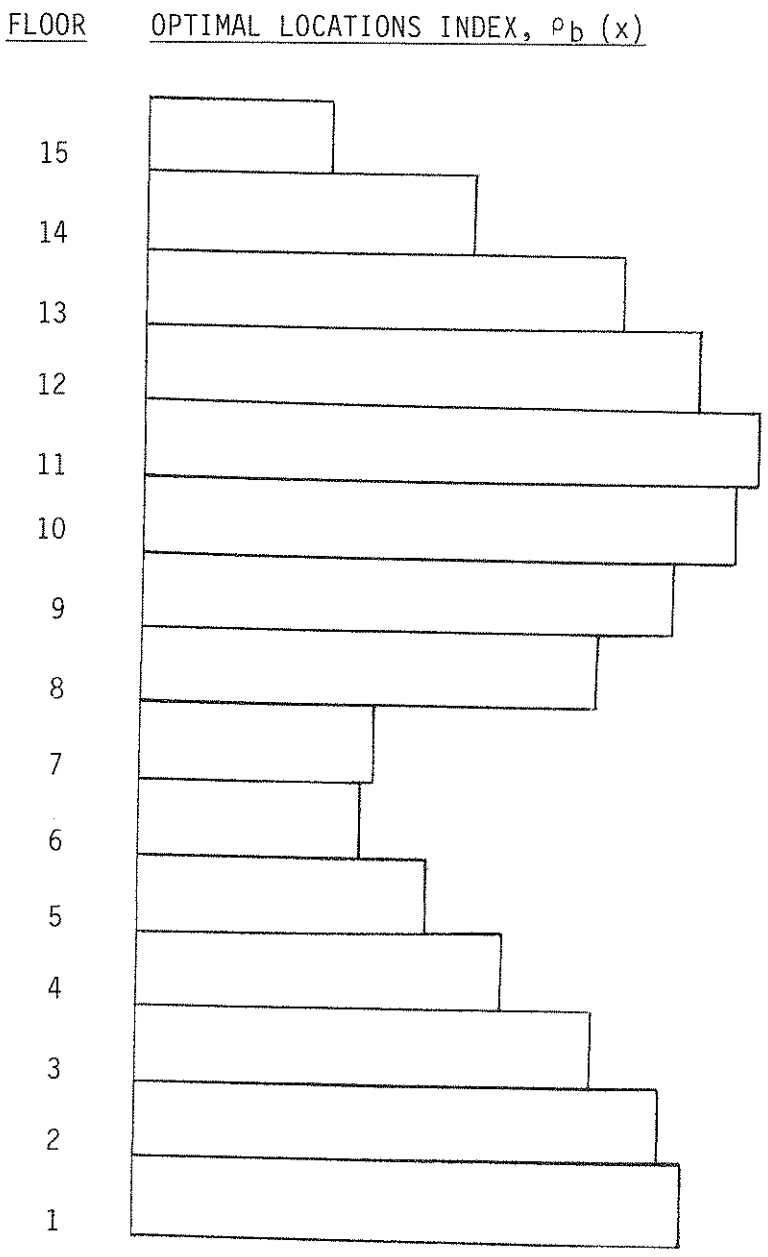

FIGURE 3-16 Optimal Locations Index for Example 6 -- Two Modes

TABLE 3-IV OPTIMAL LOCATIONS FOR EXAMPLE 6 -- HIGHER MODES

FLOOR	3 MODES	4 MODES	5 MODES
	$\rho_b(x)$	$\rho_b(x)$	$\rho_b(x)$
1	7.27	7.36	7.361
2	6.41	6.44	6.443
3	4.88	4.88	4.884
4	3.65	3.75	3.752
5	3.95	4.13	4.136
6	4.88	5.00	5.004
7	5.57	5.59	5.590
8	8.18	8.20	8.197
9	6.80	6.91	6.908
10	5.90	6.05	6.052
11	6.88	6.93	6.927
12	8.39	8.39	8.392
13	4.84	4.96	4.962
14	7.28	7.41	7.414
15	4.22	4.33	4.335

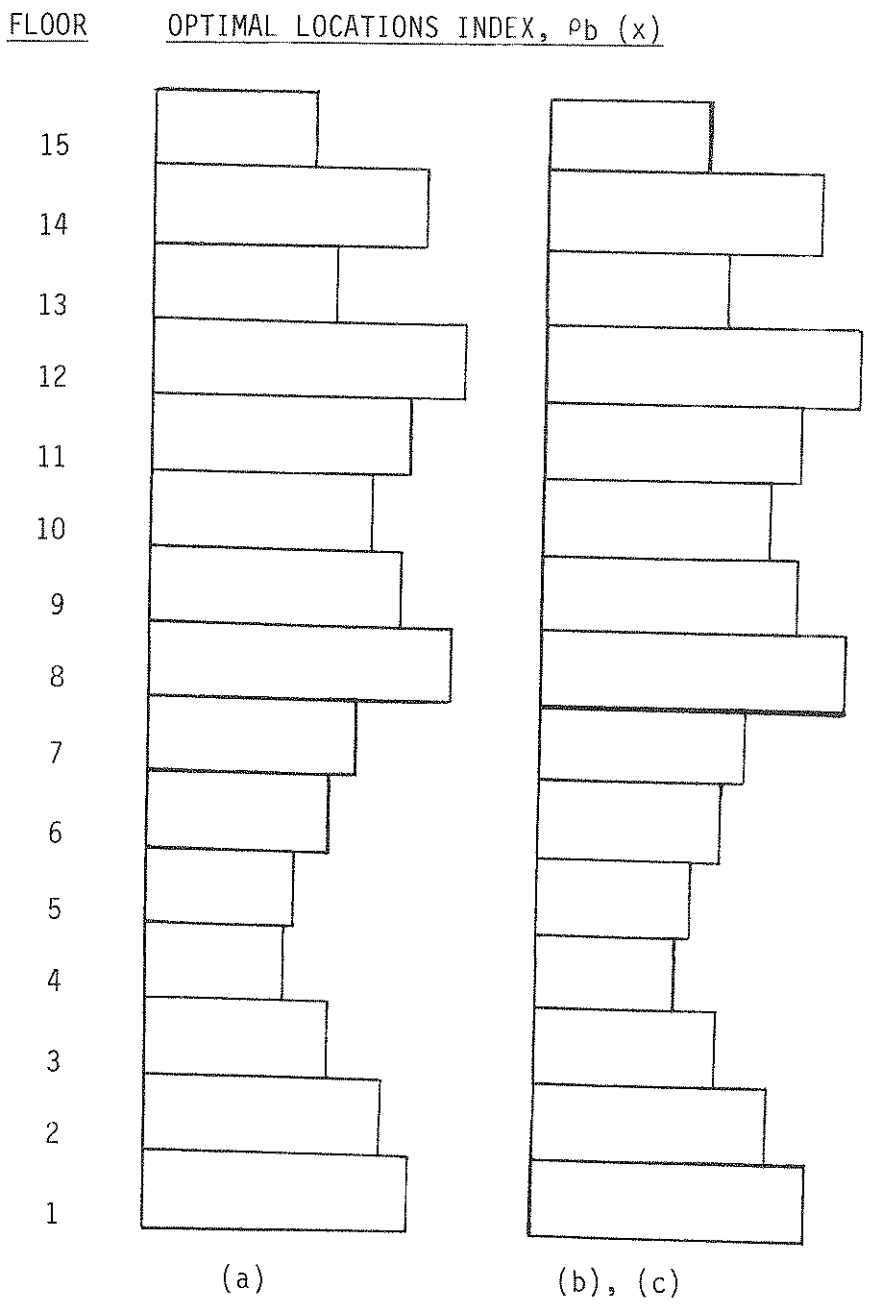

FIGURE 3-17 Optimal Locations Index for Example 6 -- Higher Modes: (a) Three Modes, (b) Four Modes, (c) Five Modes

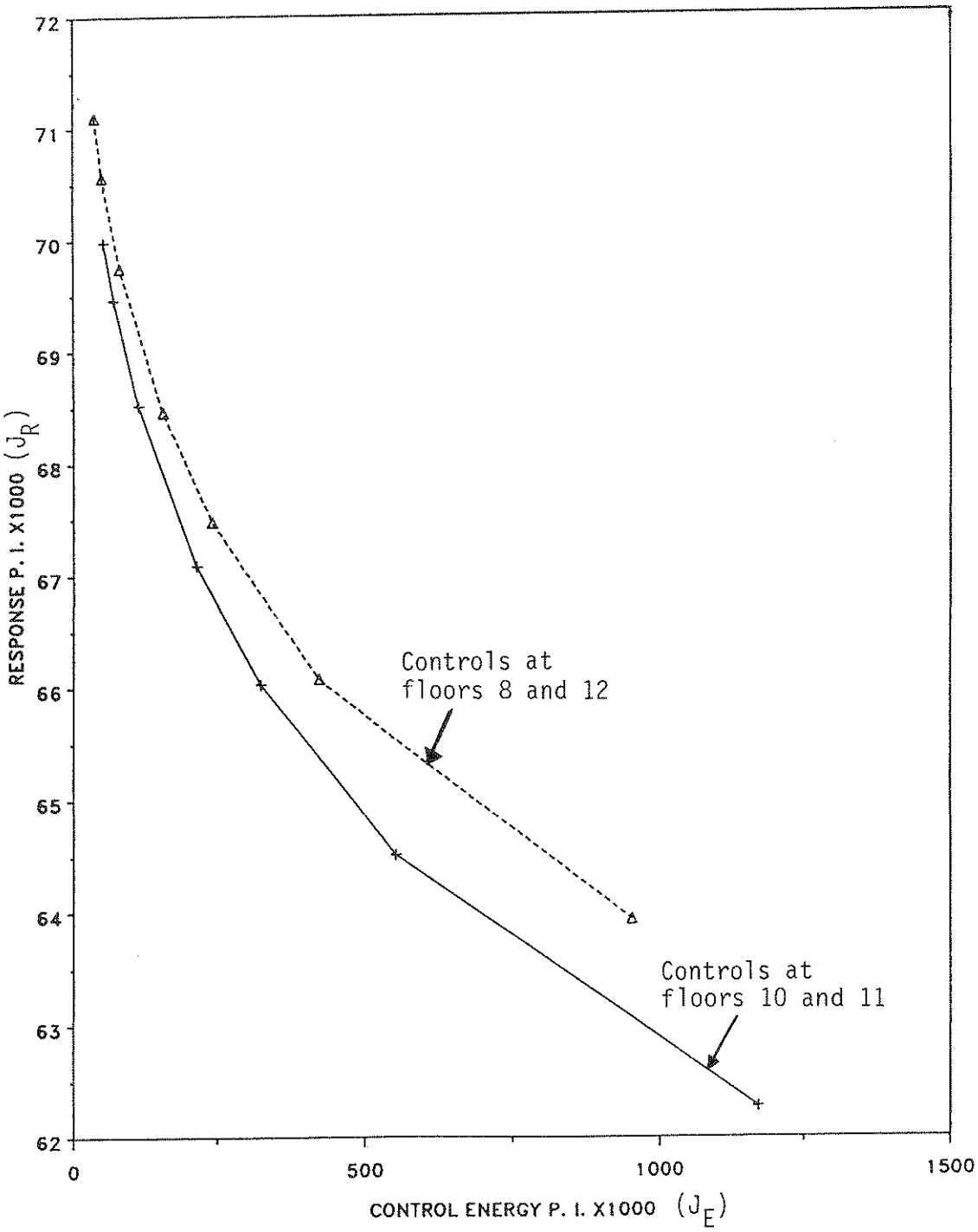

FIGURE 3-18 Control Energy and Response Performance Indices for Example 6 -- Two Modes

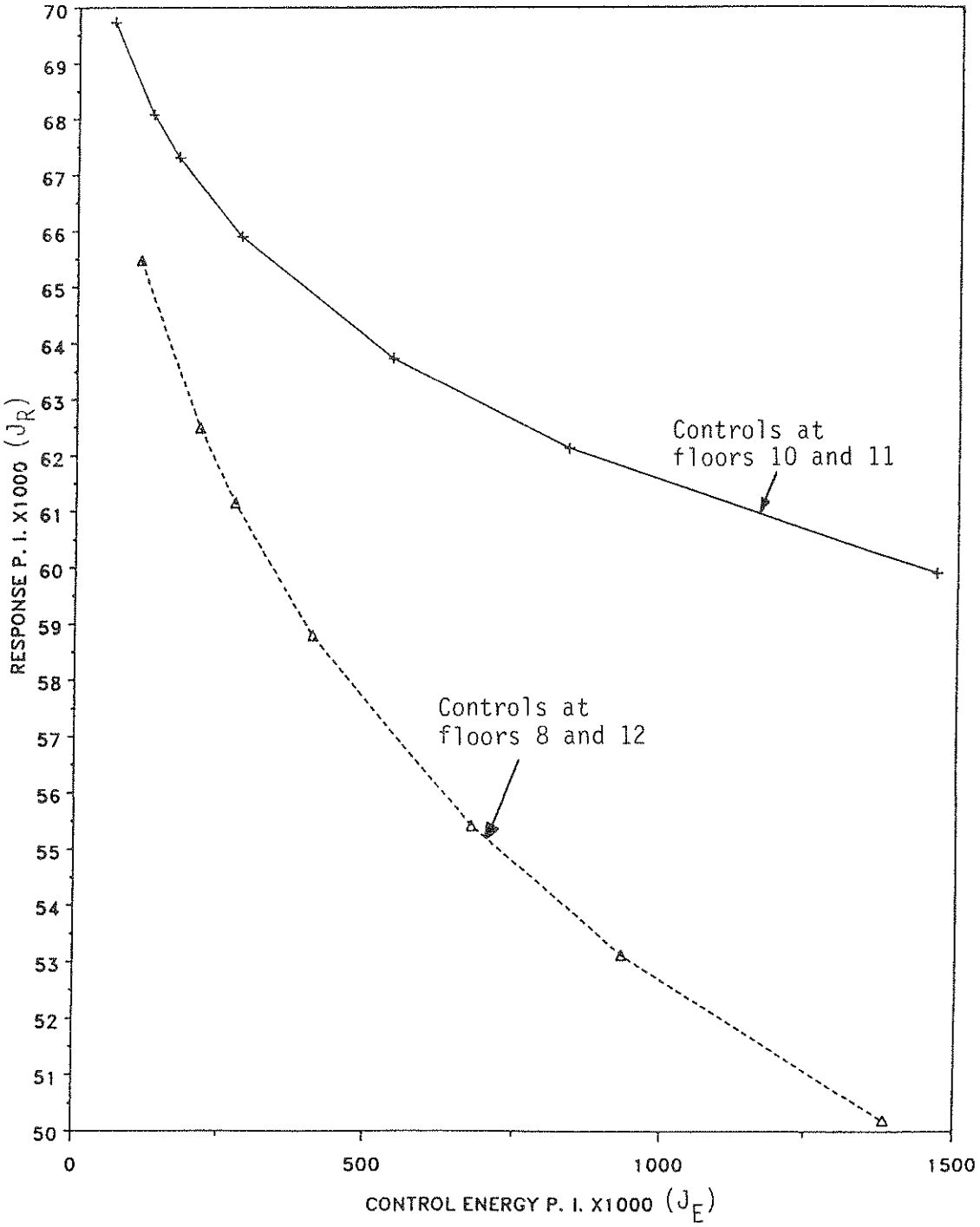

FIGURE 3-19 Control Energy and Response Performance Indices for Example 6 -- Five Modes

3.3.6 Example 7: Validation of Controllability Index as Optimal Locations Criterion

The numerical examples presented in this section have compared two cases of interest. The control energy and response performance indices were then plotted and the prediction made by using Eq. (9) was confirmed through the plot of performance indices. In this example a comparison is made between three different cases in order to validate the controllability index as an optimal locations criterion. The data for this example are those of Example 5. The controllability index of Eq. (9) using two modes is shown on Table 3-II and Figure 3-13. The following conclusions were obtained from the controllability index $\rho_b(X)$ for two controller locations:

(a) best (floors ten and eleven)

(b) intermediate (floors one and two)

(c) worst (floors one and fifteen)

A simulation was carried out to obtain the time-history of the response to the El-Centro 1940 earthquake. The control energy and response performance indices are given in Figure 3-20 for cases (A), (B) and (C). As predicted (A) gives the least response, (B) an intermediate response and (C) the worst response, for all levels of control energy. Thus Figure 3-20 confirms the results of applying Eq. (9). Actual time-histories for the three cases are compared in Figure 3-21 for the seventh floor response, and in Figure 3-22 for the fifteenth floor response. It is observed that both figures confirm the validity of the method of using the controllability index of Eq.(9) for determining optimal locations of active controllers.

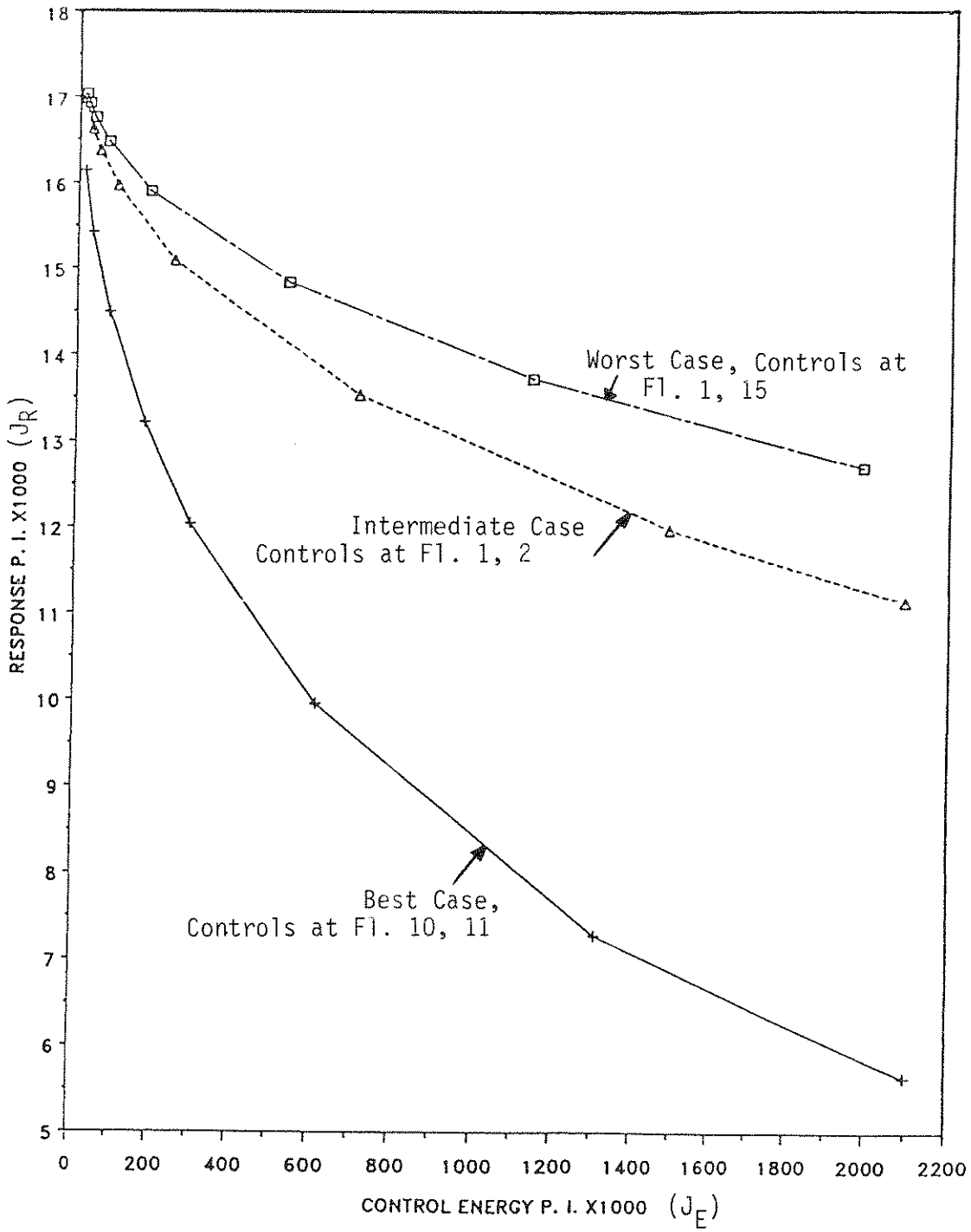

FIGURE 3-20 Control Energy and Response Performance Indices for Example 7

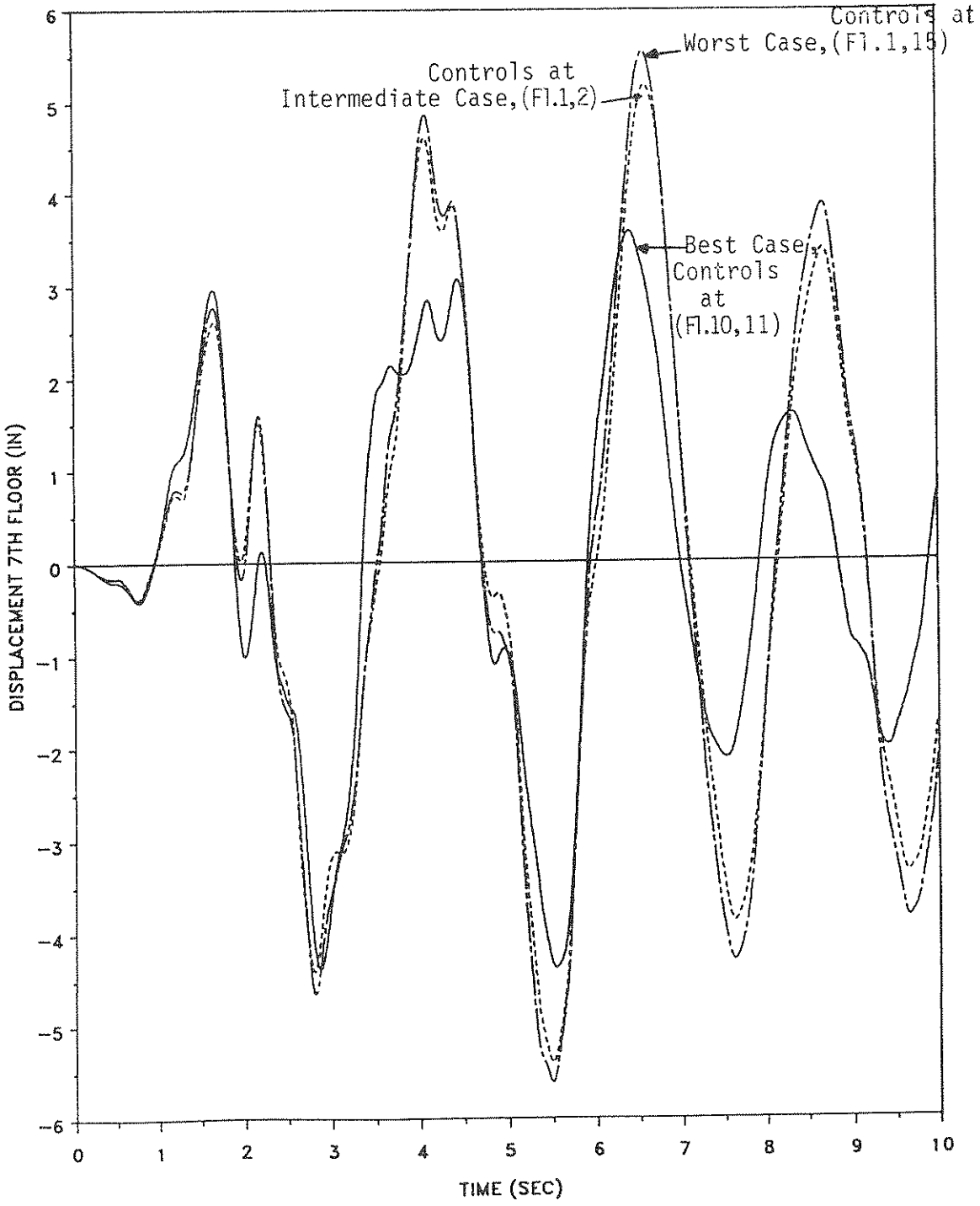

FIGURE 3-21 Displacement Response of Seventh Floor for Example 7

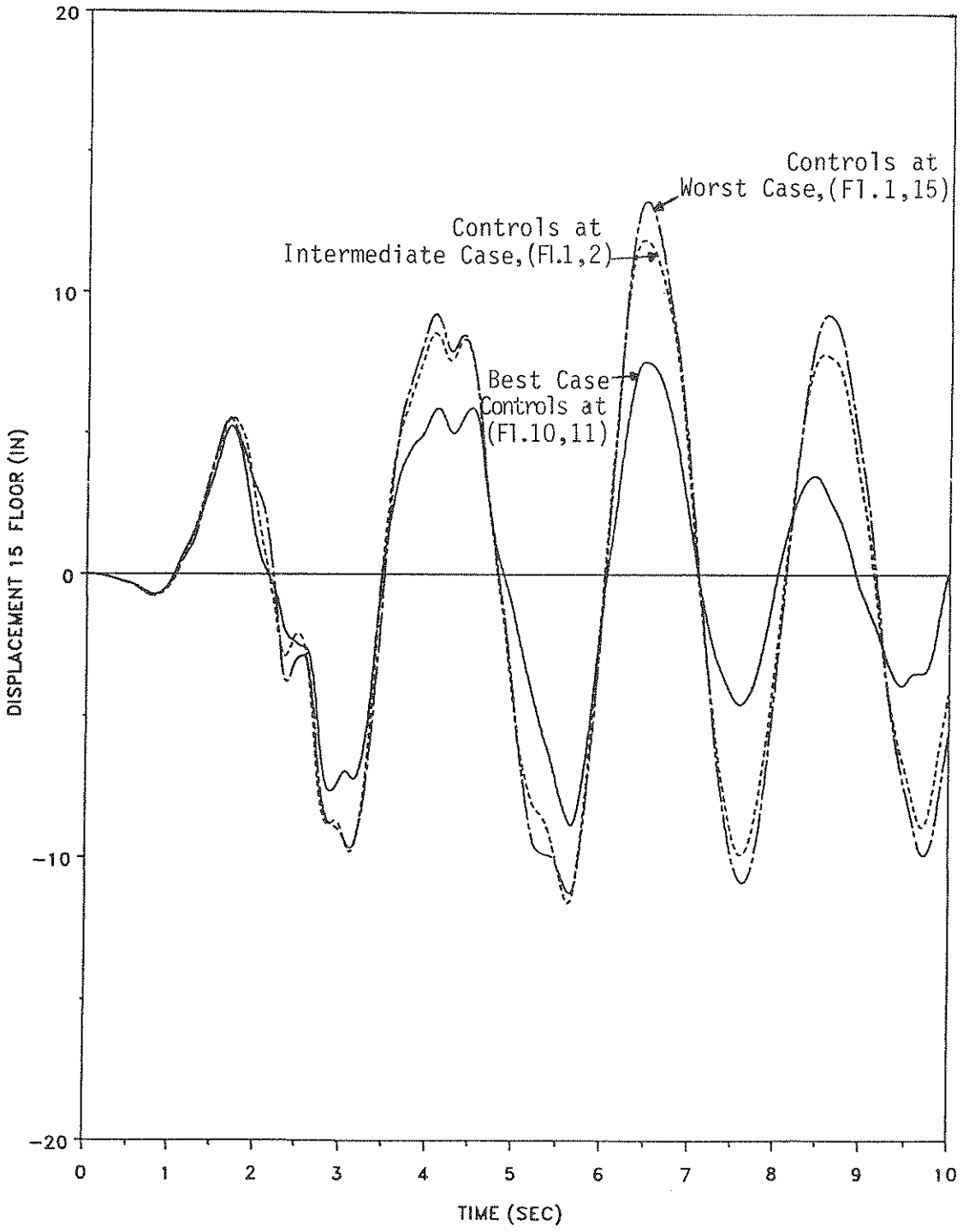

FIGURE 3-22 Displacement Response of Fifteenth Floor for Example 7

SECTION 4 CONCLUSIONS

A method of scalar index for determining the optimal locations of active tendons for seismic structures is developed on the basis of the concept of degree of controllability for free vibrations. The method considers the mode-shapes of the structure and weights the response in a root-mean-square fashion in order to arrive at locations with maximum index; these locations are considered optimal. The optimal locations found using the method satisfy the requirement of minimum control energy, which is reflected in the control energy performance index.

The method is in agreement with the method of control energy and response performance indices. The latter method however needs a lot of computation time because a random search is required to determine the candidate locations. Investigations of the mode-shapes of a structure (not equipped with control) show that they are sufficient for evaluating the scalar index and that considering the mode-shapes of the controlled structure does not affect the results. The optimal locations of active tendons were found to remain optimal for two different earthquakes.

The optimal locations index depends on the structural parameters of the building. A building of the same height with different structural properties has different optimal locations for active tendons. Studies of how many modes are sufficient in using the method, showed that the procedure can be terminated when an increase in the number of modes considered does not alter the optimal locations. The usefulness of the method is

demonstrated when categories of best, intermediate and worst selections for optimal locations are verified.

SECTION 5

APPENDIX A

TABLE 5-I OPTIMAL LOCATIONS INDEX USING PROPOSED METHOD - EXAMPLE 1

X_1	$\lvert\varphi_1\rvert$	$\lvert\varphi_2\rvert$	$\rho_a(x_1)$=OLI
0.0	0.000	0.000	0.000
0.1	0.046	0.182	0.020
0.2	0.174	0.591	0.072
0.3	0.372	1.033	0.148
0.4	0.626	1,347	0.241
0.5	0.925	1.401	0.347
0.6	1,256	1,157	0.463
0.7	1.610	0.623	0.588
0.8	1.976	0.137	0.721
0.9	2.349	1.029	0.859
1.0	2.724	1.964	1.000

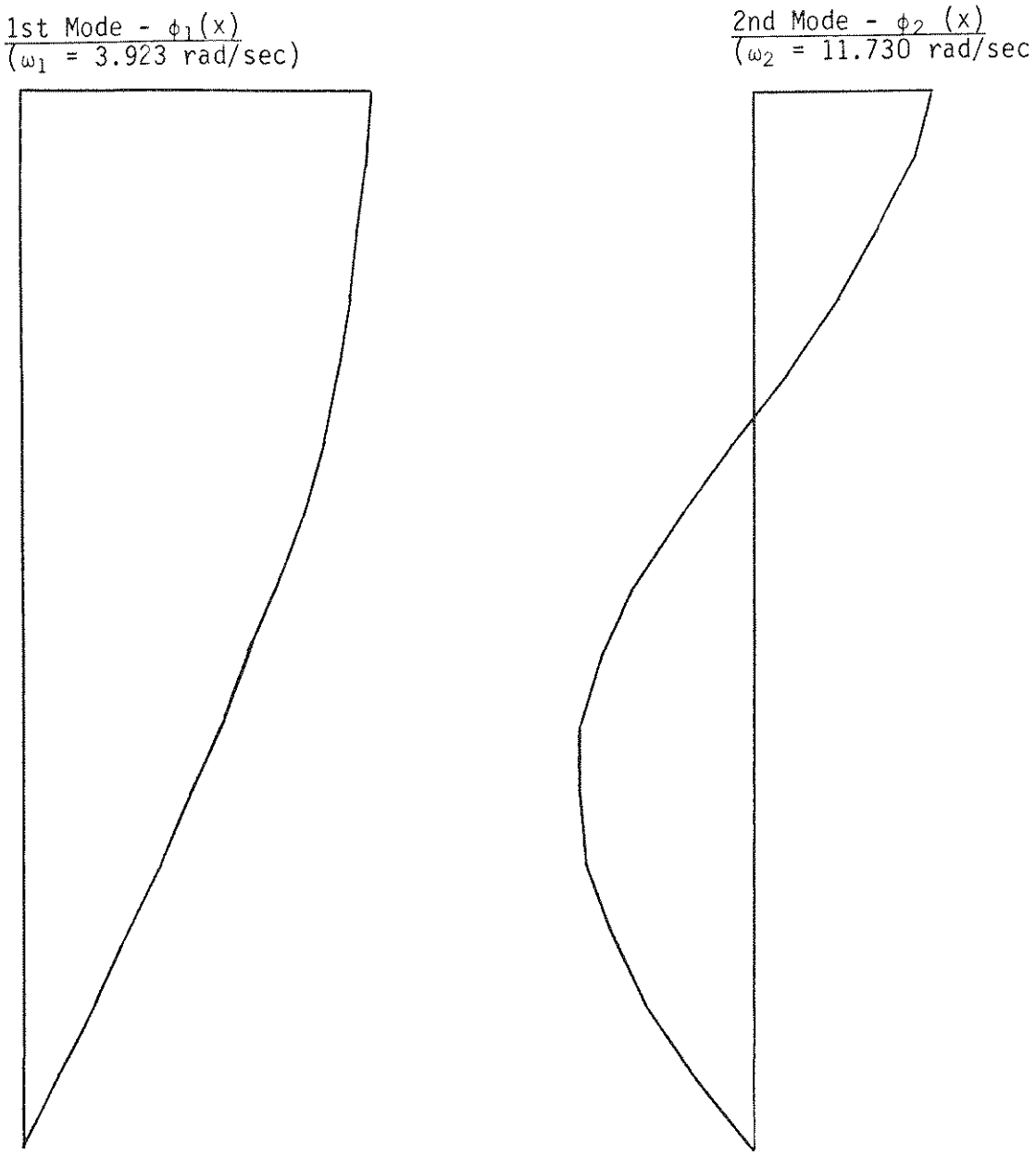

FIGURE 5-1 Mode Shapes of Example 2

TABLE 5-II OPTIMAL LOCATIONS USING COMPLEX MODES OF EXAMPLE 3

Floor	X_1	φ_1	φ_2	$\Delta\varphi_1/\Delta X_1$	$\Delta\varphi_2/\Delta X_1$	$\rho_b(X_1)$
1	.067	-.001834-.025766i	-.003151-.024536i	.390	.375	6.04
2	.133	-.003617-.051317i	-.005974-.046907i	.375	.330	5.69
3	.200	-.004338-.076337i	-.005457-.065211i	.375	.270	5.48
4	.267	-.004998-.100578i	-.004615-.077544i	.375	.195	5.26
5	.333	-.005639-.123802i	-.003596-.082845i	.345	.075	4.66
6	.400	-.006209-.145723i	-.002401-.080325i	.330	.045	4.43
7	.467	-.006738-.166170i	-.001225-.070538i	.300	.135	4.16
8	.533	-.007216-.184904i	-.000119-.054262i	.285	.255	4.34
9	.600	-.007645-.201744i	.000852-.032982i	.255	.315	4.26
10	.667	-.008018-.216518i	.001665-.008683i	.225	.360	4.19
11	.733	-.008335-.229068i	.002288+.016392i	.180	.390	3.97
12	.800	-.008590-.239264i	.002749+.039978i	.150	.345	3.44
13	.867	-.008780-.247005i	.003071+.059882i	.120	.300	2.91
14	.933	-.008910-.252214i	.003252+.074234i	.075	.210	1.97
15	1.000	-.008969-.254830i	.003347+.081778i	.045	.120	1.14

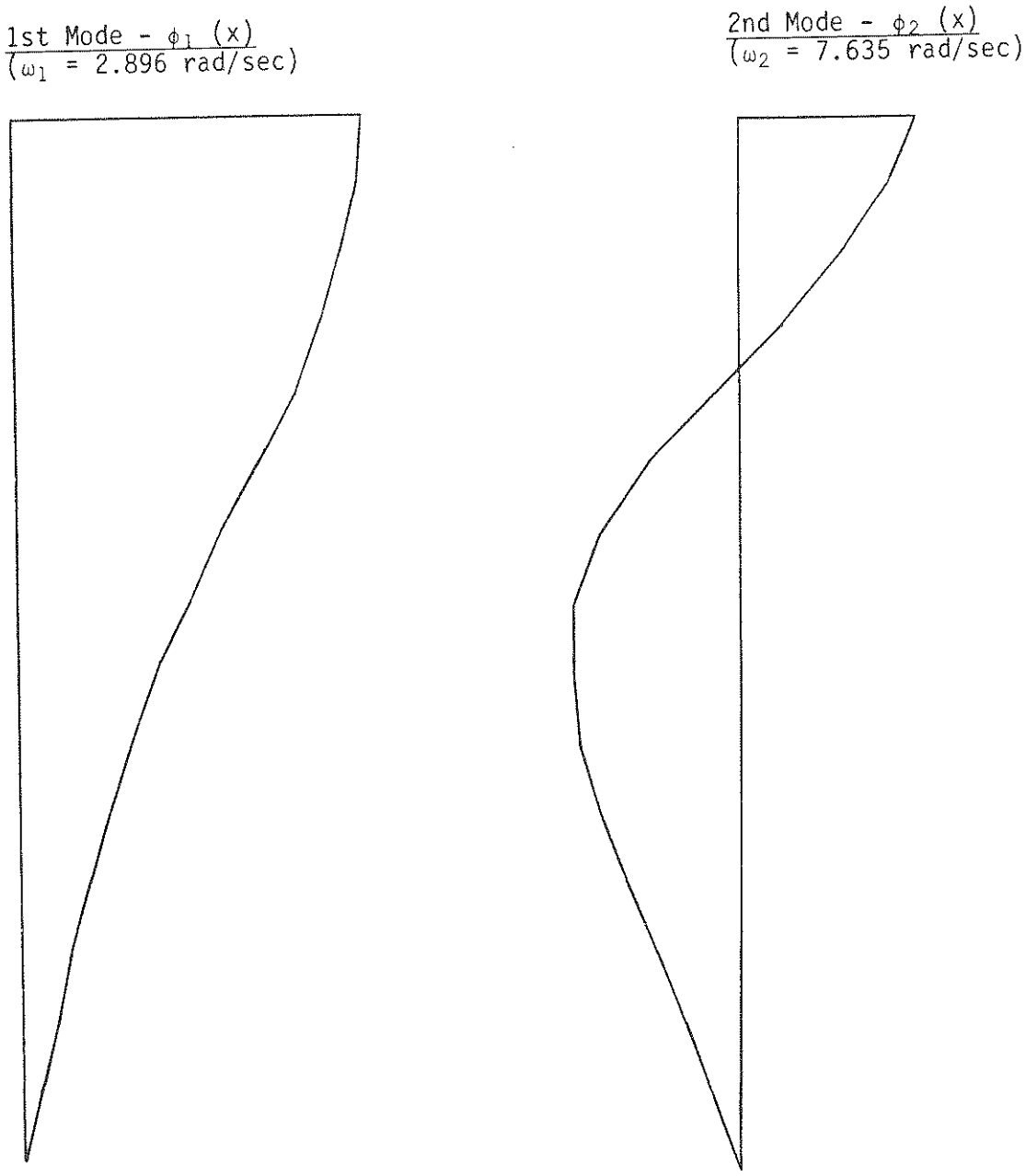

FIGURE 5-2 Mode Shapes of Example 5

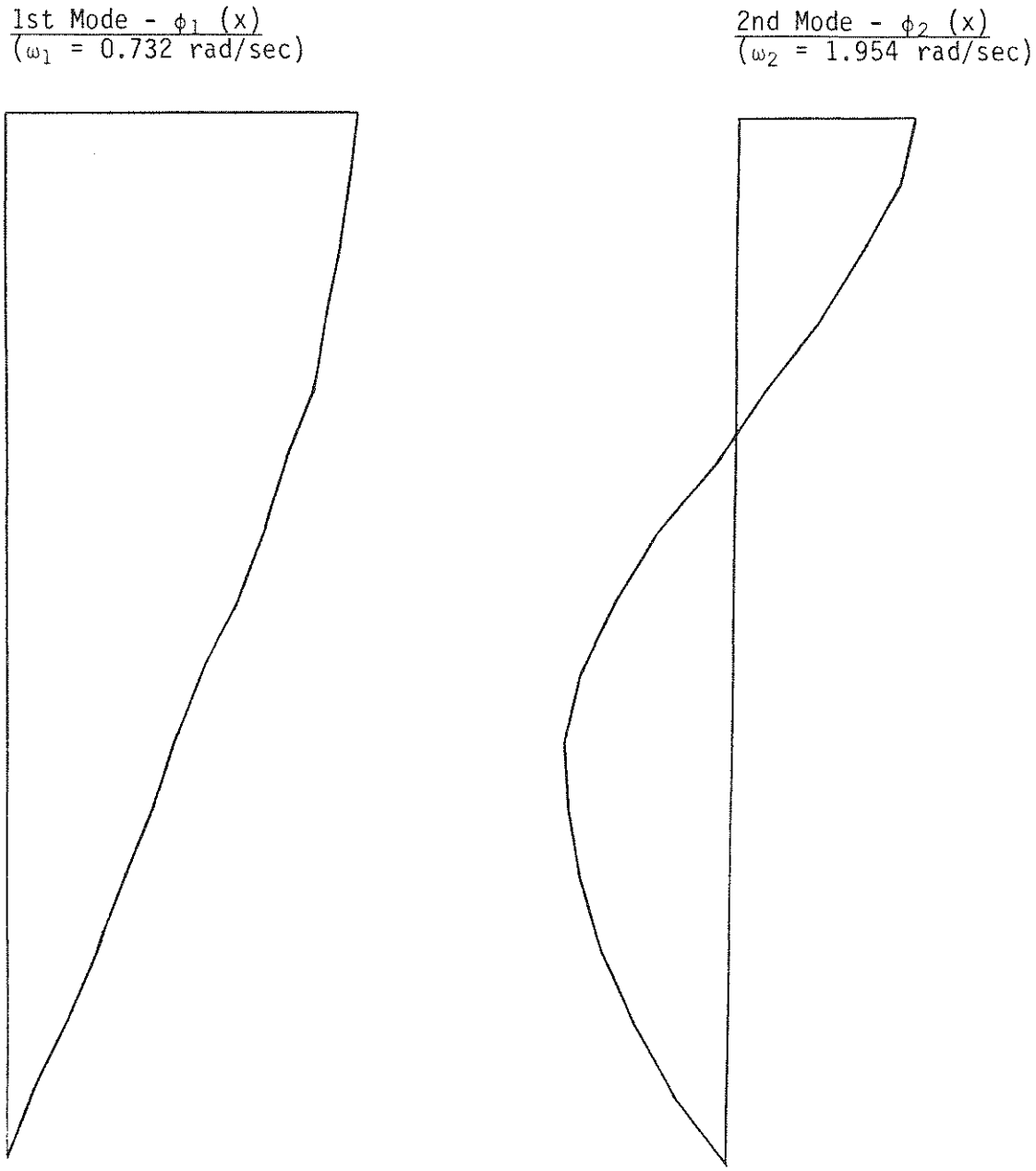

FIGURE 5-3 Mode Shapes of Example 6

SECTION 6

REFERENCES

1. Lin, R.C., Soong, T.T. and Reinhorn, A.M., "Experimental Evaluation of Instantaneous Optimal Algorithms for Structural Control", 4/20/87, Technical Report, NCEER-87-0002.

2. Chung, L.L., Reinhorn, A.M. and Soong, T.T., "An Experimental Study of Active Structural Control", Dynamic Response of Structures, G.C. Hart and R.B. Nelson, Eds., ASCE, New York, N.Y., pp. 795-802, 1986.

3. Masri, S.F., Bekey, G.A. and Caughey, T.K. "Optimum Pulse Control of Flexible Structures", J. of Appl. Mechanics, ASME Transactions, Vol. 48, pp. 619-626, 1981.

4. Martin, C.R. and Soong, T.T., "Modal Control of Multistory Structures", J. Engrg. Mech. Div., ASCE, Vol. 102, No. EM4, pp. 613-623, 1976.

5. Laskin, R.A., "Aspects of the Dynamics and Controllability of Large Flexible Structures", Ph.D. Dissertation, Columbia University, N.Y., 1982.

6. Lindberg, R.E. Jr. and Longman, R.W., "On the Number and Placement of Actuators for Independent Modal Space Control", J. Guidance, Vol. 7, No. 2, pp. 215-221, March-April, 1984.

7. Vander Velde, W.E. and Carignan, C.R., "Number and Placement of Control System Components Considering Possible Gailures", J. Guidance, Vol. 7, No. 6, pp. 703-709, Nov-Dec., 1984.

8. Ibidapo-Obe, O., "Optimal Actuators Placements for the Active Control of Flexible Structures", J. of Math. Analysis and Applications, 105, No. 1, pp. 12-25, Jan. 1985.

9. Cheng, F.Y., and Pantelides, C.P., "Combining Structural Optimization and Structural Control", 1/10/88, Technical Report, NCEER-88-0006.

NATIONAL CENTER FOR EARTHQUAKE ENGINEERING RESEARCH
LIST OF PUBLISHED TECHNICAL REPORTS

The National Center for Earthquake Engineering Research (NCEER) publishes technical reports on a variety of subjects related to earthquake engineering written by authors funded through NCEER. These reports are available from both NCEER's Publications Department and the National Technical Information Service (NTIS). Requests for reports should be directed to the Publications Department, National Center for Earthquake Engineering Research, State University of New York at Buffalo, Red Jacket Quadrangle, Buffalo, New York 14261. Reports can also be requested through NTIS, 5285 Port Royal Road, Springfield, Virginia 22161. NTIS accession numbers are shown in parenthesis, if available.

NCEER-87-0001 "First-Year Program in Research, Education and Technology Transfer," 3/5/87, (PB88-134275/AS).

NCEER-87-0002 "Experimental Evaluation of Instantaneous Optimal Algorithms for Structural Control," by R.C. Lin, T.T. Soong and A.M. Reinhorn, 4/20/87, (PB88-134341/AS).

NCEER-87-0003 "Experimentation Using the Earthquake Simulation Facilities at University at Buffalo," by A.M. Reinhorn and R.L. Ketter, to be published.

NCEER-87-0004 "The System Characteristics and Performance of a Shaking Table," by J.S. Hwang, K.C. Chang and G.C. Lee, 6/1/87, (PB88-134259/AS).

NCEER-87-0005 "A Finite Element Formulation for Nonlinear Viscoplastic Material Using a Q Model," by O. Gyebi and G. Dasgupta, 11/2/87, (PB88-213764/AS).

NCEER-87-0006 "Symbolic Manipulation Program (SMP) - Algebraic Codes for Two and Three Dimensional Finite Element Formulations," by X. Lee and G. Dasgupta, 11/9/87, (PB88-219522/AS).

NCEER-87-0007 "Instantaneous Optimal Control Laws for Tall Buildings Under Seismic Excitations," by J.N. Yang, A. Akbarpour and P. Ghaemmaghami, 6/10/87, (PB88-134333/AS).

NCEER-87-0008 "IDARC: Inelastic Damage Analysis of Reinforced Concrete Frame - Shear-Wall Structures," by Y.J. Park, A.M. Reinhorn and S.K. Kunnath, 7/20/87, (PB88-134325/AS).

NCEER-87-0009 "Liquefaction Potential for New York State: A Preliminary Report on Sites in Manhattan and Buffalo," by M. Budhu, V. Vijayakumar, R.F. Giese and L. Baumgras, 8/31/87, (PB88-163704/AS). This report is available only through NTIS (see address given above).

NCEER-87-0010 "Vertical and Torsional Vibration of Foundations in Inhomogeneous Media," by A.S. Veletsos and K.W. Dotson, 6/1/87, (PB88-134291/AS).

NCEER-87-0011 "Seismic Probabilistic Risk Assessment and Seismic Margins Studies for Nuclear Power Plants," by Howard H.M. Hwang, 6/15/87, (PB88-134267/AS). This report is available only through NTIS (see address given above).

NCEER-87-0012 "Parametric Studies of Frequency Response of Secondary Systems Under Ground-Acceleration Excitations," by Y. Yong and Y.K. Lin, 6/10/87, (PB88-134309/AS).

NCEER-87-0013 "Frequency Response of Secondary Systems Under Seismic Excitation," by J.A. HoLung, J. Cai and Y.K. Lin, 7/31/87, (PB88-134317/AS).

NCEER-87-0014 "Modelling Earthquake Ground Motions in Seismically Active Regions Using Parametric Time Series Methods," by G.W. Ellis and A.S. Cakmak, 8/25/87, (PB88-134283/AS).

NCEER-87-0015 "Detection and Assessment of Seismic Structural Damage," by E. DiPasquale and A.S. Cakmak, 8/25/87, (PB88-163712/AS).

NCEER-87-0016 "Pipeline Experiment at Parkfield, California," by J. Isenberg and E. Richardson, 9/15/87, (PB88-163720/AS).

NCEER-87-0017 "Digital Simulation of Seismic Ground Motion," by M. Shinozuka, G. Deodatis and T. Harada, 8/31/87, (PB88-155197/AS). This report is available only through NTIS (see address given above).

NCEER-87-0018 "Practical Considerations for Structural Control: System Uncertainty, System Time Delay and Truncation of Small Control Forces," J.N. Yang and A. Akbarpour, 8/10/87, (PB88-163738/AS).

NCEER-87-0019 "Modal Analysis of Nonclassically Damped Structural Systems Using Canonical Transformation," by J.N. Yang, S. Sarkani and F.X. Long, 9/27/87, (PB88-187851/AS).

NCEER-87-0020 "A Nonstationary Solution in Random Vibration Theory," by J.R. Red-Horse and P.D. Spanos, 11/3/87, (PB88-163746/AS).

NCEER-87-0021 "Horizontal Impedances for Radially Inhomogeneous Viscoelastic Soil Layers," by A.S. Veletsos and K.W. Dotson, 10/15/87, (PB88-150859/AS).

NCEER-87-0022 "Seismic Damage Assessment of Reinforced Concrete Members," by Y.S. Chung, C. Meyer and M. Shinozuka, 10/9/87, (PB88-150867/AS). This report is available only through NTIS (see address given above).

NCEER-87-0023 "Active Structural Control in Civil Engineering," by T.T. Soong, 11/11/87, (PB88-187778/AS).

NCEER-87-0024 Vertical and Torsional Impedances for Radially Inhomogeneous Viscoelastic Soil Layers," by K.W. Dotson and A.S. Veletsos, 12/87, (PB88-187786/AS).

NCEER-87-0025 "Proceedings from the Symposium on Seismic Hazards, Ground Motions, Soil-Liquefaction and Engineering Practice in Eastern North America," October 20-22, 1987, edited by K.H. Jacob, 12/87, (PB88-188115/AS).

NCEER-87-0026 "Report on the Whittier-Narrows, California, Earthquake of October 1, 1987," by J. Pantelic and A. Reinhorn, 11/87, (PB88-187752/AS). This report is available only through NTIS (see address given above).

NCEER-87-0027 "Design of a Modular Program for Transient Nonlinear Analysis of Large 3-D Building Structures," by S. Srivastav and J.F. Abel, 12/30/87, (PB88-187950/AS).

NCEER-87-0028 "Second-Year Program in Research, Education and Technology Transfer," 3/8/88, (PB88-219480/AS).

NCEER-88-0001 "Workshop on Seismic Computer Analysis and Design of Buildings With Interactive Graphics," by W. McGuire, J.F. Abel and C.H. Conley, 1/18/88, (PB88-187760/AS).

NCEER-88-0002 "Optimal Control of Nonlinear Flexible Structures," by J.N. Yang, F.X. Long and D. Wong, 1/22/88, (PB88-213772/AS).

NCEER-88-0003 "Substructuring Techniques in the Time Domain for Primary-Secondary Structural Systems," by G.D. Manolis and G. Juhn, 2/10/88, (PB88-213780/AS).

NCEER-88-0004 "Iterative Seismic Analysis of Primary-Secondary Systems," by A. Singhal, L.D. Lutes and P.D. Spanos, 2/23/88, (PB88-213798/AS).

NCEER-88-0005 "Stochastic Finite Element Expansion for Random Media," by P.D. Spanos and R. Ghanem, 3/14/88, (PB88-213806/AS).

NCEER-88-0006 "Combining Structural Optimization and Structural Control," by F.Y. Cheng and C.P. Pantelides, 1/10/88, (PB88-213814/AS).

NCEER-88-0007 "Seismic Performance Assessment of Code-Designed Structures," by H.H-M. Hwang, J-W. Jaw and H-J. Shau, 3/20/88, (PB88-219423/AS).

NCEER-88-0008 "Reliability Analysis of Code-Designed Structures Under Natural Hazards," by H.H-M. Hwang, H. Ushiba and M. Shinozuka, 2/29/88, (PB88-229471/AS).

NCEER-88-0009 "Seismic Fragility Analysis of Shear Wall Structures," by J-W Jaw and H.H-M. Hwang, 4/30/88.

NCEER-88-0010 "Base Isolation of a Multi-Story Building Under a Harmonic Ground Motion - A Comparison of Performances of Various Systems," by F-G Fan, G. Ahmadi and I.G. Tadjbakhsh, 5/18/88.

NCEER-88-0011 "Seismic Floor Response Spectra for a Combined System by Green's Functions," by F.M. Lavelle, L.A. Bergman and P.D. Spanos, 5/1/88.

NCEER-88-0012 "A New Solution Technique for Randomly Excited Hysteretic Structures," by G.Q. Cai and Y.K. Lin, 5/16/88.

NCEER-88-0013 "A Study of Radiation Damping and Soil-Structure Interaction Effects in the Centrifuge," by K. Weissman, supervised by J.H. Prevost, 5/24/88.

NCEER-88-0014 "Parameter Identification and Implementation of a Kinematic Plasticity Model for Frictional Soils," by J.H. Prevost and D.V. Griffiths, to be published.

NCEER-88-0015 "Two- and Three- Dimensional Dynamic Finite Element Analyses of the Long Valley Dam," by D.V. Griffiths and J.H. Prevost, 6/17/88.

NCEER-88-0016 "Damage Assessment of Reinforced Concrete Structures in Eastern United States," by A.M. Reinhorn, M.J. Seidel, S.K. Kunnath and Y.J. Park, 6/15/88.

NCEER-88-0017 "Dynamic Compliance of Vertically Loaded Strip Foundations in Multilayered Viscoelastic Soils," by S. Ahmad and A.S.M. Israil, 6/17/88.

NCEER-88-0018 "An Experimental Study of Seismic Structural Response With Added Viscoelastic Dampers," by R.C. Lin, Z. Liang, T.T. Soong and R.H. Zhang, 6/30/88.

NCEER-88-0019 "Experimental Investigation of Primary - Secondary System Interaction," by G.D. Manolis, G. Juhn and A.M. Reinhorn, 5/27/88.

NCEER-88-0020 "A Response Spectrum Approach For Analysis of Nonclassically Damped Structures," by J.N. Yang, S. Sarkani and F.X. Long, 4/22/88.

NCEER-88-0021 "Seismic Interaction of Structures and Soils: Stochastic Approach," by A.S. Veletsos and A.M. Prasad, 7/21/88.

NCEER-88-0022 "Identification of the Serviceability Limit State and Detection of Seismic Structural Damage," by E. DiPasquale and A.S. Cakmak, 6/15/88.

NCEER-88-0023 "Multi-Hazard Risk Analysis: Case of a Simple Offshore Structure," by B.K. Bhartia and E.H. Vanmarcke, 7/21/88.

NCEER-88-0024 "Automated Seismic Design of Reinforced Concrete Buildings," by Y.S. Chung, C. Meyer and M. Shinozuka, 7/5/88.

NCEER-88-0025 "Experimental Study of Active Control of MDOF Structures Under Seismic Excitations," by L.L. Chung, R.C. Lin, T.T. Soong and A.M. Reinhorn, 7/10/88, (PB89-122600/AS).

NCEER-88-0026 "Earthquake Simulation Tests of a Low-Rise Metal Structure," by J.S. Hwang, K.C. Chang, G.C. Lee and R.L. Ketter, 8/1/88.

NCEER-88-0027 "Systems Study of Urban Response and Reconstruction Due to Catastrophic Earthquakes," by F. Kozin and H.K. Zhou, 9/22/88, to be published.

NCEER-88-0028 "Seismic Fragility Analysis of Plane Frame Structures," by H.H-M. Hwang and Y.K. Low, 7/31/88.

NCEER-88-0029 "Response Analysis of Stochastic Structures," by A. Kardara, C. Bucher and M. Shinozuka, 9/22/88, to be published.

NCEER-88-0030 "Nonnormal Accelerations Due to Yielding in a Primary Structure," by D.C.K. Chen and L.D. Lutes, 9/19/88.

NCEER-88-0031 "Design Approaches for Soil-Structure Interaction," by A.S. Veletsos, A.M. Prasad and Y. Tang, to be published.

NCEER-88-0032 "A Re-evaluation of Design Spectra for Seismic Damage Control," by C.J. Turkstra and A.G. Tallin, 11/7/88.

NCEER-88-0033 "The Behavior and Design of Noncontact Lap Splices Subjected to Repeated Inelastic Tensile Loading," by V.E. Sagan, P. Gergely and R.N. White, to be published.

NCEER-88-0034 "Seismic Response of Pile Foundations," by S.M. Mamoon, P.K. Banerjee and S. Ahmad, 11/1/88.

NCEER-88-0035 "Modeling of R/C Building Structures With Flexible Floor Diaphragms (IDARC2)," by A.M. Reinhorn, S.K. Kunnath and N. Panahshahi, 9/7/88, to be published.

NCEER-88-0036 "Solution of the Dam-Reservoir Interaction Problem Using a Combination of Fem, Bem with Particular Integrals, Modal Analysis, and Subtracting," by C-S. Tsai, G.C. Lee and R.L. Ketter, 12/88, to be published.

NCEER-88-0037 "Optimal Placement of Actuators for Structural Control," by F.Y. Cheng and C.P. Pantelides, 8/15/88.